

Fig. 3. mIEF (a) and cIEF (b) for profiling of charge variants of transferrin under optimized conditions. Peaks were labeled as T1 through T5 depending on their detection positions in mIEF. Smaller peak number means more acidic peak in the test sample. Analytical conditions for mIEF are the same as those in Fig. 2. Analytical conditions for cIEF: capillary, DB-1 capillary (Agilent Technologies), 50 μm I.D. with an effective length of 30 cm (total length, 40 cm); anolyte, 0.2 mol/L phosphoric acid with 0.4% HPMC; catholyte, 0.3 mol/L sodium hydroxide with 0.4% HPMC; injection, 2 min at 30 psi; focusing, 25 kV in normal polarity for 10 min; mobilization, 25 kV in normal polarity with pressure at 0.5 psi on both negative and positive ends of capillary; temperature, 20 °C; detection, UV at 280 nm.

transferrin in the presence of urea at high concentrations [36]. In the analysis of transferrin, urea is not necessary (Fig. 2d–1).

TEMED is often used as an additive for preventing focusing of basic proteins beyond the detection window in cIEFs and works as a spacer between the catholyte and the basic end of pH gradient [35,37]. However, addition of TEMED in the separation mixture at 0.4% concentration obviously decreased resolution (data not shown). Thus, TEMED is not necessary in the analysis of isoforms of transferrin in mIEF. However, in case of the analysis of basic proteins having higher pI values ($pI > 10$), TEMED is required as a spacer.

Based on the optimization studies on the analysis of transferrin, the sample solution was prepared as follows: 2.4% of Pharmalyte (5–8:3–10, 19:1), 0.2% of HPMC and 2 mg/mL of transferrin.

3.1.4. Analysis of isoforms of transferrin by mIEF and cIEF

Under the optimized conditions, transferrin was resolved into 5 isoforms within 200 s in a range of 5–15 mm from the anolyte reservoir (Fig. 3a). pI Values of the peaks were calculated by linear regression between pI 5.12 and 7.40 markers. Calculated pI value of the most abundant isoform (T4) was 6.06, and other isoforms (T1, T2, T3, and T5) were observed between pI 5.46 and 6.19 in mIEF analysis.

The calculated pI values obtained by mIEF were compared with those acquired by cIEF as shown in Fig. 3b. The difference (ΔpI) of calculated pI values of the most abundant isoform (T4) was +0.14

(Table 3). And those of other isoforms (T1, T2, T3 and T5) ranged from -0.08 to $+0.19$. Thus, calculated pI values obtained by mIEF were comparable to those obtained by cIEF.

Sensitivities of the proposed mIEF system were slightly lower than those of cIEF system (see Fig. 3). The limit of detection (LOD) for transferrin (isoform T4) in mIEF was estimated to be ca. 0.2 mg/mL (as final concentration) from a signal to noise ratio ($S/N=3$). On the other hand, LOD in cIEF was 0.005 mg/mL. Because the total length of the channel is 25 mm in mIEF, the amount of the injected sample is much smaller than cIEF. This is the major reason why high sensitivity is not achieved in mIEF. However, the proposed mIEF with linear imaging UV detection system does not need sample mobilization toward detection window which often causes diffusion of focused charge variants and disruption of pH gradient. Furthermore, we can monitor the progress of separations in the real-time manner, therefore, readily find the optimal conditions (see the movie for the analysis of transferrin in electronic supplementary materials).

3.1.5. Effect of the presence of arginine in the sample solution

Most isoforms of mAb preparations show pI values between pI 7 and pI 10. Prior to the analysis of mAb, pH gradient formed during mIEF was examined using four pI markers (pI s 7.40, 8.18, 9.22, and 10.10) for accurate determination of pI values [5]. mIEF separation was performed using a mixture prepared by 2.4 μL of pharmalyte 8–10.5, 34 μL of 0.6% HPMC, 1 μL of each pI marker,

Table 3
Comparisons of calculated pI values in mIEF and cIEF.

Peak number	pI values in mIEF (ΔpI)			
	Transferrin	Bevacizumab	Trastuzumab	Cetuximab
1 (acidic end)	5.46 (-0.08)	7.96 ($+0.09$)	8.45 (-0.07)	7.57 (-0.12)
2	5.70 (± 0.00)	8.10 ($+0.07$)	8.57 (-0.05)	7.71 (-0.16)
3	5.88 ($+0.06$)	8.29 ($+0.05$)	8.76 ($+0.02$)	7.90 (-0.14)
4	6.06 ($+0.14$)	8.41 (-0.01)	8.89 ($+0.04$)	8.09 (-0.15)
5	6.19 ($+0.19$)	–	8.98 ($+0.03$)	8.26 (-0.16)
6	–	–	–	8.43 (-0.18)
7	–	–	–	8.57 (-0.19)
8 (basic end)	–	–	–	8.68 (-0.25)

pI values obtained by mIEF are shown in the table. Numbers shown in round bracket are the actual pI difference (ΔpI) compared with those obtained by conventional cIEF method. Peaks observed in each sample were labeled depending on their detection positions as shown in Figs. 3 and 5. Peak 1 means the most acidic-end peak in the sample, but they were not identical charge variants among the tested samples.

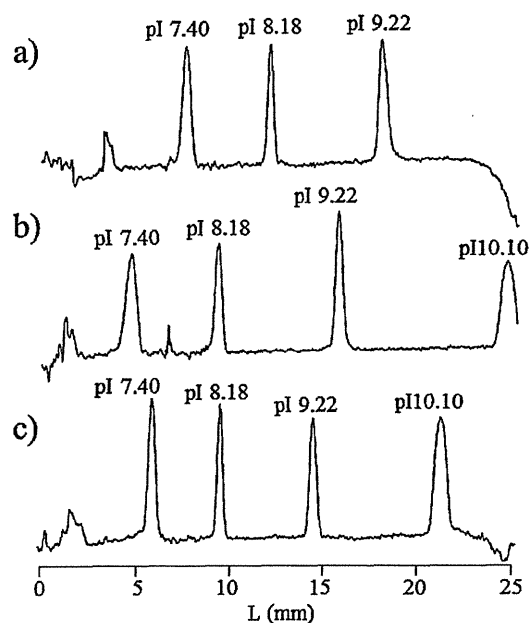


Fig. 4. mIEF separations of the mixture of four pI markers (pI 7.40, 8.18, 9.22, and 10.10) in the presence of (a) 0.0 mmol/L, (b) 4 mmol/L, and (c) 8 mmol/L arginine. Analytical conditions are the same as those in Fig. 2.

several volume of 200 mmol/L of arginine (pI = 10.76) which is commonly used as cathodic stabilizer [9] and water to make the sample solution to 100 μ L. When analyzing the four pI markers without arginine, pI 10.10 marker was not detected due to leakage from the cathodic end (Fig. 4a). Addition of arginine to the mixture induced pI shift toward anodic end due to accumulated arginine zone at the cathodic end (Fig. 4b), and addition of 8 mmol/L of arginine showed the best separation of four pI markers within 240 s (Fig. 4c). Good linear relationship ($R^2 = 0.983$) was observed between the pI values and distances of the pI markers from the anolyte reservoir.

3.2. mIEF analysis of mAb pharmaceuticals

The optimized conditions employed for the analysis of transferrin was applied to the analysis of commercially available mAb products (bevacizumab, trastuzumab, and cetuximab). The analytical conditions were slightly modified based on the pI values of each mAb preparation.

For mIEF of mAb products, the mixture containing 2.4% phar-malyte 8–10.5, 0.2% HPMC, 8 mmol/L arginine and 2 mg/mL mAbs with two pI markers (pI 7.40 and 10.10) was employed as the sam-ple solution. In bevacizumab, four charge variants (peak b1 to b4) were observed in both mIEF (Fig. 5a) and cIEF (Fig. 5b). pI values calculated by linear regression are summarized in Table 3. Δ pI values were less than 0.09 for all observed peaks. And, relative abundances of the peaks (b1, b2, b3, and b4) were 4.0%, 23.5%, 69.2%, and 3.3% for mIEF, and were well correlated with the data observed by cIEF (5.0%, 24.9%, 64.8%, and 5.2%).

Other mAb products, trastuzumab (Fig. 5c) and cetuximab (Fig. 5e), were separated into five and eight charge variants by mIEF. Both electropherograms showed consistent profiles with those obtained by cIEF (Fig. 5d and f). The present data indicate that the proposed mIEF method is comparable to cIEF, and shows excellent ability in high-speed mAb analysis.

Table 4
Intra- and inter-day assay variations of mIEF.

	Calculated pI values			
	b1	b2	b3	b4
<i>Repeatability (intra-day)</i>				
1	7.86	8.03	8.25	8.45
2	7.83	8.00	8.22	8.42
3	7.86	8.03	8.22	8.44
Mean	7.85	8.02	8.23	8.44
RSD (%)	0.22	0.22	0.21	0.21
<i>Reproducibility (inter-day)</i>				
Day 1-1	7.86	8.02	8.22	8.43
Day 1-2	7.83	8.00	8.21	8.40
Day 1-3	7.86	8.04	8.22	8.43
Day 2-1	7.85	8.05	8.25	8.46
Day 2-2	7.86	8.05	8.23	8.46
Day 2-3	7.84	8.02	8.25	8.44
Day 3-1	7.86	8.03	8.25	8.45
Day 3-2	7.83	8.00	8.22	8.42
Day 3-3	7.86	8.03	8.22	8.45
Mean	7.85	8.03	8.23	8.44
RSD (%)	0.17	0.23	0.19	0.24

Peaks observed in bevacizumab were labeled as b1 through b4 depending on their detection positions as shown in Fig. 5a.

3.3. Precision of mIEF method

In order to evaluate the precision of the optimized mIEF method, repeatability and reproducibility were investigated using bevacizumab as a model mAb product. For repeatability assessment, a single separation mixture was prepared and analyzed using two pI markers of 7.40 and 9.22 instead of 10.10. On the other hand, for reproducibility assessment, separation mixtures were prepared in triplicate on each day, and analyzed by mIEF over three days as summarized in Table 4.

All four charge variants were separated each other within 380 s, and RSDs of the measured position (L , mm) ranged from 0.81% to 1.28% under optimized conditions (data not shown). After correction using pI markers, RSDs of calculated pI values were less than 0.25%. These values were comparable with those obtained by icIEF (0.2% or less in [15,38]). These data indicate that the proposed mIEF method shows excellent reproducibility, because the method does not require mobilization, and superior to those obtained by the conventional two-step cIEF [5]. In addition, RSDs of relative abundances of each peak (b1 to b4) in repeatability experiments (intra-day, $n=3$) were 9.5%, 0.7%, 1.7%, and 11.5%, and in reproducibility executions (inter-day, $n=9$) were 14.0%, 8.8%, 3.8%, and 16.6%, respectively. These values were similar to those reported previously using icIEF as described above.

3.4. Assessment of heterogeneity by sequential enzymatic digestions of mAb pharmaceuticals

C-Terminal lysine variants [39] and the presence of sialo N-glycans in mAb products [40] are the major reasons for charge variants. Two enzymes, carboxypeptidase B and sialidase, were used to understand charge heterogeneity of cetuximab. Digestion of cetuximab with carboxypeptidase B caused disappearance of two peaks (c7 and c8) at basic region (Fig. 6b).

In contrast, trastuzumab and bevacizumab (humanized antibody products manufactured by CHO cells) showed no significant changes (data not shown). These results are consistent with the previous report that relative amounts of incorporated C-terminal lysine in mAbs manufactured by CHO cell lines were up to 5% [40]. In addition, further digestion with sialidase resulted in

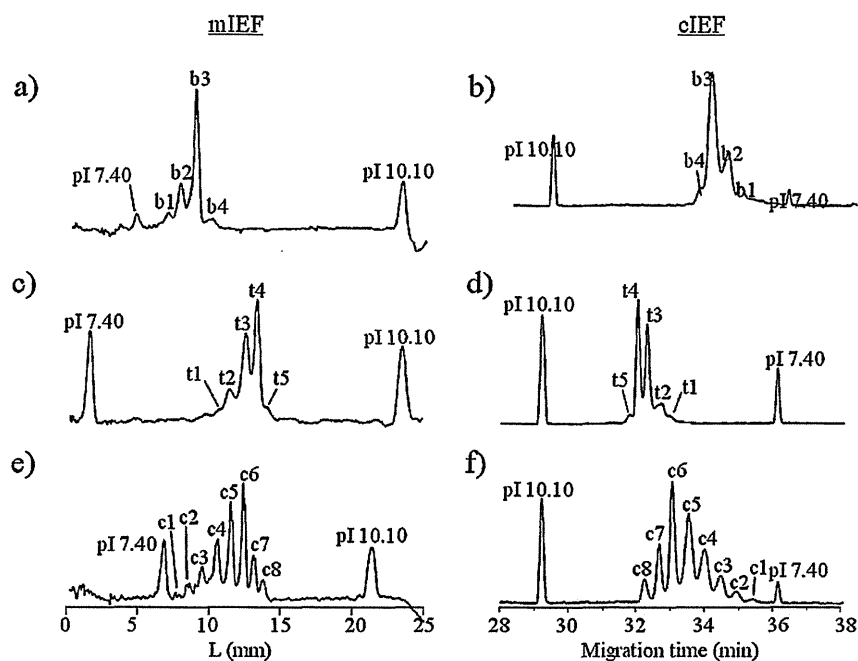


Fig. 5. Analysis of charge variants of bevacizumab, trastuzumab, and cetuximab by mIEF (left column) and cIEF (right column). Peaks observed in each sample were labeled with numbers depending on their detection positions. Peak 1 means the most acidic-end peak in the sample, but they were not identical charge variants among the tested samples. Analytical conditions are the same as shown in Fig. 2. Bevacizumab (a and b), trastuzumab (c and d) and cetuximab (e and f).

decrease/disappearance of the peaks observed in acidic *pI* regions (Fig. 6c). After successive digestion with these two enzymes, cetuximab gave the simple profile which is similar to that of bevacizumab and trastuzumab as shown in Fig. 5a and c. Thus, charge heterogeneity of cetuximab is largely due to C-terminal lysine processing and sialylation of *N*-glycans. These charge heterogeneities of cetuximab may be due to manufacturing process. Bevacizumab and trastuzumab are humanized mAb products (IgG₁), and produced by

CHO cells. In contrast, cetuximab is chimeric mouse-human IgG₁ produced by mouse myeloma SP2/0 cell line. This means that manufacturing process change in cell type may lead significant alteration in mAb heterogeneity especially in charge variants. Several charge variants are still present in enzyme-treated cetuximab. Although cetuximab may include other possible modifications such as *N*-terminal glutamine cyclization, asparagine deamination, and methionine oxidation, detailed structural analysis will be necessary to get better understanding in heterogeneity of mAbs by analyzing fractionated peaks such as accurate mass spectrometric methods.

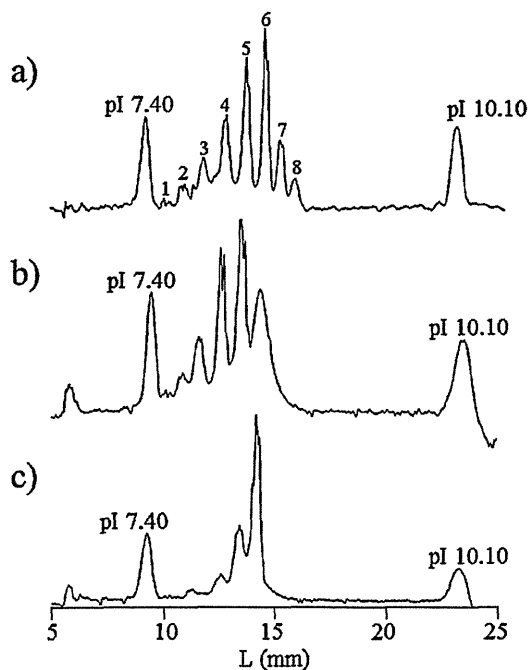


Fig. 6. mIEF separation of (a) intact, (b) carboxypeptidase B-treated, and (c) sialidase-treated cetuximab. Analytical conditions are the same as shown in Fig. 2.

4. Conclusion

A combination of a quartz chip specialized for isoelectric focusing and a microchip electrophoresis system with a whole column imaging UV photodiode array detector achieved ultrafast evaluation of charge variants of glycoproteins. The quartz chip having a simple, short and straight channel without any coating could resolve transferrin and three mAb pharmaceuticals into their charge variants within 200 s and 380 s with high reproducibility in terms of calculated *pI* values and percent relative amounts of each charge variant.

Charge profiles of protein samples determined by mIEF well corresponded to those obtained by cIEF. When comparing precision in *pI* determination in mIEF measurements with icIEF measurements (e.g. commercially available iCE280 Analyzer), and cIEF, reproducibility of the calculated *pI* values is comparable to the iCE280 and superior to cIEF [15,38]. It should be noted that the time required for the analysis is much shorter than cIEF (approximately 10 times), which requires mobilization step after completion of focusing, and faster than icIEF (about 3 times) due to incorporation of shorter separation channel. Whole column imaging UV photodiode array detector leads precise tuning of focusing time, because the progress of the focusing can be monitored on the real-time basis. However, the proposed system needs to wash the chip manually, and further improvements in functionalization and

automation will be required for commercial use in the pharmaceutical industries. It is difficult to introduce enough amount of the sample due to short analytical channel. Improvement of the sensitivity is another future requirement.

Evaluation of charge heterogeneity is necessary for assurance of quality and stability of mAb products. Some charge variants derived from several post-translational modifications or degradation show different biological activity and stability compared to their original variants [41,42]. Isoelectric focusing based techniques such as mIEF, icIEF and cIEF makes us easy to access to useful information on product specific “fingerprint” derived from charge heterogeneity of biopharmaceuticals. To get much better understanding in detail into the therapeutics, further investigation such as structural analyses, potency, toxicity and stability evaluation will be required. Mass spectrometry is one of the powerful tools to satisfy these demands from the pharmaceutical industry, and fractionated/separated peaks need to be analyzed for further evaluation of their characterization.

The proposed ultrafast and precise mIEF method is easily applied to identity and purity analyses in product lot release, stability testing, formulation screening, process development, comparability assessment and product characterization of biopharmaceutical products possessing complex charge heterogeneity.

Acknowledgements

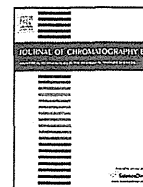
The authors would like to thank Dr. Eiki Maeda at Analytical Development Laboratories, CMC Center, Takeda Pharmaceutical Company Limited for experimental supports. The authors are also grateful to Shin Nakamura and Akihiro Arai at Life Science Business Department, Analytical & Measuring Instruments Division, Shimadzu Cooperation for providing microchip and measuring equipment.

Appendix A. Supplementary data

Supplementary data associated with this article can be found, in the online version, at <http://dx.doi.org/10.1016/j.chroma.2013.08.021>.

References

- [1] S.A. Berkowitz, J.R. Engen, J.R. Mazzeo, G.B. Jones, *Nat. Rev. Drug Discov.* 11 (2012) 527.
- [2] M. Mann, O.N. Jensen, *Nat. Biotechnol.* 21 (2003) 255.
- [3] O.N. Jensen, *Curr. Opin. Chem. Biol.* 8 (2004) 33.
- [4] J. Seo, K.-J. Lee, J. Biochem. Mol. Biol. 37 (2004) 35.
- [5] E. Maeda, K. Urakami, K. Shimura, M. Kinoshita, K. Kakehi, *J. Chromatogr. A* 1217 (2010) 7164.
- [6] H. Svensson, *Acta Chem. Scand.* 15 (1961) 325.
- [7] S. Hjertén, M.-d. Zhu, *J. Chromatogr.* 346 (1985) 265.
- [8] Y. Kuroda, H. Yukinaga, M. Kitano, T. Noguchi, M. Nemat, A. Shibukawa, T. Nakagawa, K. Matsuzaki, *J. Pharm. Biomed. Anal.* 37 (2005) 423.
- [9] J. Lin, Q. Tan, S. Wang, *J. Sep. Sci.* 34 (2011) 1696.
- [10] K.G. Moorhouse, C.A. Rickel, A.B. Chen, *Electrophoresis* 17 (1996) 423.
- [11] J. Wu, J. Pawliszyn, *Anal. Chem.* 64 (1992) 2934.
- [12] J. Wu, J. Pawliszyn, *Anal. Chem.* 64 (1992) 224.
- [13] P. Dou, Z. Liu, J. He, J.-J. Xu, H.-Y. Chen, *J. Chromatogr. A* 1190 (2008) 372.
- [14] X.Z. He, A.H. Que, J.J. Mo, *Electrophoresis* 30 (2009) 714.
- [15] Z. Sosic, D. Houde, A. Blum, T. Carlage, Y. Lyubarskaya, *Electrophoresis* 29 (2008) 4368.
- [16] L. Goodridge, C. Goodridge, J. Wu, M. Griffiths, J. Pawliszyn, *Anal. Chem.* 76 (2004) 48.
- [17] Z. Liu, J. Pawliszyn, *Electrophoresis* 26 (2005) 556.
- [18] M. Vlcková, F. Kalman, M.A. Schwarz, *J. Chromatogr. A* 1181 (2008) 145.
- [19] F. Kitagawa, S. Aizawa, K. Otsuka, *Anal. Sci.* 25 (2009) 979.
- [20] H. Nakanishi, T. Nishimoto, A. Arai, H. Abe, M. Kanai, Y. Fujiyama, T. Yoshida, *Electrophoresis* 22 (2001) 230.
- [21] H. Stibler, *Clin. Chem.* 37 (1991) 2029.
- [22] F. Crivellente, G. Fracasso, R. Valentini, G. Manetto, A.P. Riviera, F. Tagliaro, *J. Chromatogr. B: Biomed. Sci. Appl.* 739 (2000) 81.
- [23] F. Tagliaro, F. Bortolotti, M. Zuliani, F. Crivellente, G. Manetto, V.L. Pascali, M. Marigo, *J. Capill. Electrophor. Microchip Technol.* 6 (1999) 137.
- [24] F. Tagliaro, F. Crivellente, G. Manetto, P. Puppi, Z. Deyl, M. Marigo, *Electrophoresis* 19 (1998) 3033.
- [25] E. Landberg, E. Aström, B. Kågedal, P. Pålsson, *Clin. Chim. Acta: Int. J. Clin. Chem.* 414C (2012) 58.
- [26] S.R. Bean, G.L. Lookhart, *Electrophoresis* 19 (1998) 3190.
- [27] P.G. Righetti, C. Gelfi, B. Verzola, L. Castelletti, *Electrophoresis* 22 (2001) 603.
- [28] M. Viefhues, S. Manchanda, T.-C. Chao, D. Anselmetti, J. Regtmeier, *A. Ros. Anal. Bioanal. Chem.* 401 (2011) 2113.
- [29] B. Deng, N. Ye, G. Luo, Y. Wang, J. Nanosci. Nanotechnol. 5 (2005) 1193.
- [30] M.-Y. Ye, X.-F. Yin, Z.-L. Fang, *Anal. Bioanal. Chem.* 381 (2005) 820.
- [31] T. Yasui, M. Reza Mohamadi, N. Kaji, Y. Okamoto, M. Tokeshi, Y. Baba, *Biomechanics* 5 (2011) 441141.
- [32] A.E. Barron, D.S. Soane, H.W. Blanch, *J. Chromatogr. A* 652 (1993) 3.
- [33] E. Quintana, R. Montero, M. Casado, A. Navarro-Sastre, M.A. Vilaseca, P. Briones, R. Artuch, *J. Chromatogr. B: Anal. Technol. Biomed. Life Sci.* 877 (2009) 2513.
- [34] S. Mack, I. Cruzado-Park, J. Chapman, C. Ratnayake, G. Vigh, *Electrophoresis* 30 (2009) 4049.
- [35] A. Cifuentes, M.V. Moreno-Arribas, M. de Frutos, J.C. Diez-Masa, *J. Chromatogr. A* 830 (1999) 453.
- [36] A. Pantazaki, M. Taverna, C. Vidal-Madjar, *Anal. Chim. Acta* 383 (1999) 137.
- [37] A. Bossi, P.G. Righetti, C. Visco, U. Breme, M. Mauriello, B. Valsasina, G. Orsini, E. Wenisch, *Electrophoresis* 17 (1996) 932.
- [38] N. Li, K. Kessler, L. Bass, D. Zeng, *J. Pharm. Biomed. Anal.* 43 (2007) 963.
- [39] L.W. Dick, D. Qiu, D. Mahon, M. Adamo, K.-C. Cheng, *Biotechnol. Bioeng.* 100 (2008) 1132.
- [40] E. Maeda, S. Kita, M. Kinoshita, K. Urakami, T. Hayakawa, K. Kakehi, *Anal. Chem.* 84 (2012) 2373.
- [41] G. Janini, N. Saptharishi, M. Waselus, G. Soman, *Electrophoresis* 23 (2002) 1605.
- [42] P.A. Trail, H.D. King, G.M. Dubowchik, *Cancer Immunol. Immunother.* 52 (2003) 328.



Free glycans derived from glycoproteins present in human sera



Kinya Iwatsuka^a, Sakie Watanabe^a, Mitsuhiro Kinoshita^a, Kazuya Kamisue^a, Keita Yamada^a, Takao Hayakawa^b, Tadashi Suzuki^c, Kazuaki Kakehi^{a,*}

^a Faculty of Pharmaceutical Sciences, Kinki University, 3-4-1 Kowakae, Higashi-Osaka 577-8502, Japan

^b Pharmaceutical Research and Technology Institute, Kinki University, Kowakae 3-4-1, Higashi-osaka 577-8502, Japan

^c Glycometabolome Laboratory, Frontier Research System, RIKEN (The Institute for Physical and Chemical Research), 2-1 Hirosawa, Wako, Saitama 351-0198, Japan

ARTICLE INFO

Article history:

Received 15 December 2012

Accepted 12 March 2013

Available online 21 March 2013

Keywords:

Free glycans

Serum

Transferrin

HPLC

ESI-TOF-MS

ABSTRACT

During the course of studies on the analysis of O-glycans in biological samples, we found that significant amount of free glycans are present in normal human serum samples. The most abundant free glycan was disialo-biantennary glycan typically observed in transferrin which is one of the abundant glycoproteins found in sera. Minor glycans were also considered to be mainly due to transferrin, but some glycans were derived from mucin-type O-glycans, although the amount was quite minute. However, high mannose-type glycans could not be detected at all. Although there have been many reports on the presence of intracellular “free” N-glycans (mainly derived from high mannose-type glycans) generated either from lipid-linked oligosaccharides or from misfolded glycoproteins through endoplasmic-reticulum associated protein degradation pathway, there is little information on the presence of free glycans in extracellular matrix and biological fluids such as serum. This report is the first one which demonstrates the presence of free glycans due to glycoproteins in sera.

© 2013 Elsevier B.V. All rights reserved.

1. Introduction

There have been many reports on the presence of free glycans in cytosols, and the formation of such free glycans is an important clue for the understanding the selection of properly synthesized glycoproteins. Such free glycans found in cytosols are exclusively high mannose-type glycans having one N-acetylglucosamine (GlcNAc) residue at the reducing termini [1,2], and are formed in the cytosol by a cellular system called ERAD (endoplasmic reticulum-associated degradation) [3]. Such intracellular “free” N-glycans are generated either from lipid-linked oligosaccharides or from misfolded glycoproteins [4–7]. In both cases, occurrence of high mannose-type free glycans, which have one GlcNAc residue at their reducing ends, has been well-documented.

Little is known with regard to the accumulation of more processed, complex-type free glycans in the cytosol of mammalian cells. In our previous report on the comprehensive analysis of N-glycans in cancer cells [8], we found that significantly large amount of unusual, complex-type free N-glycans were accumulated in stomach cancer-derived cell lines, MKN7 and MKN45. It should be noticed that all the free glycans found in these cells were cleaved between the GlcNAc β 1–4GlcNAc (i.e. chitobiose) bond and a single

GlcNAc residue was present at the reducing end. In addition, most of the accumulated glycans have N-acetylneuraminic acid (NeuAc) residues at the non-reducing termini. And we showed that loss of the activity of cytosolic neuraminidase, Neu2, was responsible for the accumulation of such unusual free glycans [9].

In contrast, there is little information on the presence of free glycans in extracellular matrixes and biological fluids such as sera probably due to insufficient and poor ability to analyze minute amount of glycans. We have been developing sensitive methods for comprehensive analyses of N- and O-glycans in biological samples, especially cancer cells, tissues and serum samples [5,10–13]. During the course of studies on the analysis of O-glycans in biological samples, we found that significant amount of free glycans are present in human serum samples. This is unexpected and interesting, although it is well known that patients suffering from genetic lysosomal disorders of complex carbohydrate metabolism excrete a considerable amount of unusual oligosaccharides in urine [14–17].

Inoue et al. reported that free glycans were present in the unfertilized eggs of a fresh water trout, *Plecoglossus altivelis* [18]. The isolated glycans consist of desialylated biantennary glycans with β -Man-GlcNAc structure at their reducing termini. However, a small portion of the glycans having chitobiose (GlcNAc β 1–4-GlcNAc) structure at the reducing ends were also present. It is still not clear why and how such large amount of free glycans are accumulated in unfertilized eggs. Another important report on the presence of free glycans is the expression of free glycans in human seminal

* Corresponding author. Tel.: +80 6 6721 2332; fax: +80 6 6721 2353.
E-mail address: k.kakehi@phar.kindai.ac.jp (K. Kakehi).

plasma [19], and the structural characteristics are similar to those in human milk. But their variations are simpler than those of human milk oligosaccharides.

According to the reference search works on the presence of free glycans in sera, the present work demonstrating the presence of free glycans in sera is the first one, and will lead to a new research project on finding glycan-based disease biomarkers.

2. Materials and methods

2.1. Materials

Sephadex LH-20 and Asahi Shodex NH2P-50 4E column were obtained from GE Healthcare UK Ltd. (Buckinghamshire, UK) and Showa Denko (Minato-ku, Tokyo, Japan), respectively. Sodium cyanoborohydride and 2-aminobenzoic acid (2AA) were from Tokyo Kasei Kogyo (Chuo-Ku, Tokyo, Japan). TOYOPAK ODS-S for solid phase extraction was from Tosoh (Minato-ku, Tokyo, Japan). VIVASPIN 500 (3000 molecular weight cut off) for ultrafiltration was from Sigma–Aldrich Japan (Shinagawa-ku, Tokyo, Japan). All other reagents were of the highest grade commercially available. All aqueous solutions were prepared using water purified with a Milli-Q purification system (Millipore, Bedford, MA, USA).

2.2. Serum samples

Serum samples from healthy volunteers were obtained under the permission of the Ethics Committee of Kinki University School of Pharmacy, and used in accordance with the tenets of the Declaration of Helsinki.

2.3. Sample preparation

2.3.1. Ultrafiltration and solid-phase extraction of the serum sample

Because the serum sample contains a large amount of low-molecular-weight materials such as monosaccharides (typically glucose) and inorganic salts, and hydrophobic compounds, these materials should be removed prior to the analysis.

A serum sample (25 μ L) was centrifuged at 15,000 \times g using an ultramembrane filter (3000 molecular weight cut off) to remove the low-molecular weight materials, and concentrated to the one fourth volume. Water (150 μ L) was added to the concentrate on the membrane, and centrifuged at 15,000 \times g again. The procedures were repeated three times. The concentrated serum sample on the membrane was transferred to a new tube, and the membrane was washed with water (150 μ L) and combined with the concentrated solution. The mixture was then passed through an ODS cartridge (90 mg) which was previously washed with methanol (0.8 mL $3\times$) and water (0.8 mL $3\times$). The clean-up procedures were performed according to the method recommended by the manufacturer.

2.3.2. Total N-glycans in a serum sample

A serum sample (150 μ L) was centrifuged at 15,000 \times g using an ultramembrane filter (3000 molecular weight cut off) to remove the low-molecular weight materials, and concentrated to dryness. The dried sample was suspended in water (200 μ L) and was mixed with 10% SDS (24 μ L) and 2-mercaptoethanol (2.4 μ L). The mixture was kept in the boiling water bath for 5 min. After cooling, 10% NP40 (nonylphenol poly(ethylene glycol ether)_n) solution (24 μ L) and 1 M sodium phosphate buffer (pH 7.5, 29 μ L) were added. After addition of N-glycoamidase F (2 units), the mixture was kept at 37 °C overnight. After cooling, ethanol (695 μ L) was added and the mixture was centrifuged at 15,000 \times g for 10 min. The supernatant was collected and evaporated to dryness under reduced pressure.

2.3.3. Releasing reaction of O-glycans in mucin-type glycoproteins in serum samples

Releasing reaction of O-glycans from mucin-type glycoproteins present in serum samples was performed using the automated glycan releasing system according to the method reported previously [10].

2.3.4. Fluorescent labeling of glycans with 2AA

The sample of glycan mixture was dissolved in water (20 μ L) and 2AA solution (100 μ L) which was freshly prepared by dissolution of 2AA (15 mg) and sodium cyanoborohydride (15 mg) in methanol (500 μ L) containing 4% sodium acetate and 2% boric acid. The mixture was kept at 80 °C for 1 h, and water (20 μ L) and 50% (v/v) methanol (200 μ L) were added to the mixture after cooling, and centrifuged at 15,000 \times g for 10 min. The supernatant solution was applied to a column of Sephadex LH-20 (1.0 cm i.d., 30 cm length), which was previously equilibrated with 50% methanol. The earlier eluted fluorescent fractions were pooled and evaporated to dryness under reduced pressure. The residue was further purified by solid phase extraction as described above (Section 2.3.1), and evaporated to dryness.

2.3.5. Digestion of the glycan mixture with neuraminidase

Neuraminidase (1 munit, 2 μ L) was added to the mixture of 2AA-labeled glycans in 20 mM acetate buffer (pH 5.0, 20 μ L), and the mixture was incubated at 37 °C overnight. After keeping the mixture in the boiling water bath for 10 min followed by centrifugation, the supernatant solution was used for MS analysis.

2.4. HPLC analysis of 2AA-labeled free glycans and N-glycans in serum samples

Analysis of the 2AA-labeled glycans was performed with two Shimadzu LC-10ADvp pumps, a Jasco FP-920 fluorescence detector equipped with a polymer-based Asahi Shodex NH2P-50 4E column (4.6 mm i.d. \times 250 mm). Linear gradient method was employed by 2% acetic acid in acetonitrile (solvent A) and 5% acetic acid in water containing 3% triethylamine (solvent B). The column was initially equilibrated and eluted with 30% solvent B for 2 min. Then, solvent B was increased to 95% over 80 min, and kept at this composition for further 20 min. The column effluent was monitored by a fluorescence detector set at an excitation wavelength of 350 nm and 425 nm for emission.

2.5. Liquid chromatography–electrospray ionization ion-trap time-of-flight mass spectrometry (LC–ESI–IT–TOF MS)

Negative electrospray ionization (ESI)–MS analyses were conducted with an LC–IT–TOF MS instrument (Shimadzu) connected with an HPLC system (LC-20AD pump and CBM-20A system controller; Shimadzu). The 2AA-labeled glycans were analyzed by infusion method. Isocratic elution was carried out at a flow rate of 0.2 mL/min with 50% (v/v) acetonitrile in water. The MS apparatus was operated at a probe voltage of 1.75 kV, CDL temperature of 180 °C, nebulizer gas flow of 1.5 L/min, ion accumulation time of 30 ms. MS range was from m/z 200 to 2000. CID parameters were as follows: energy, 50%; collision gas, 50%. MS data were processed with LCMS solution ver. 3.6 software (Shimadzu).

3. Results and discussion

3.1. Free glycans in serum samples

Fig. 1a shows the results on the analysis of O-glycans in a serum sample. In this analysis, O-glycans were previously

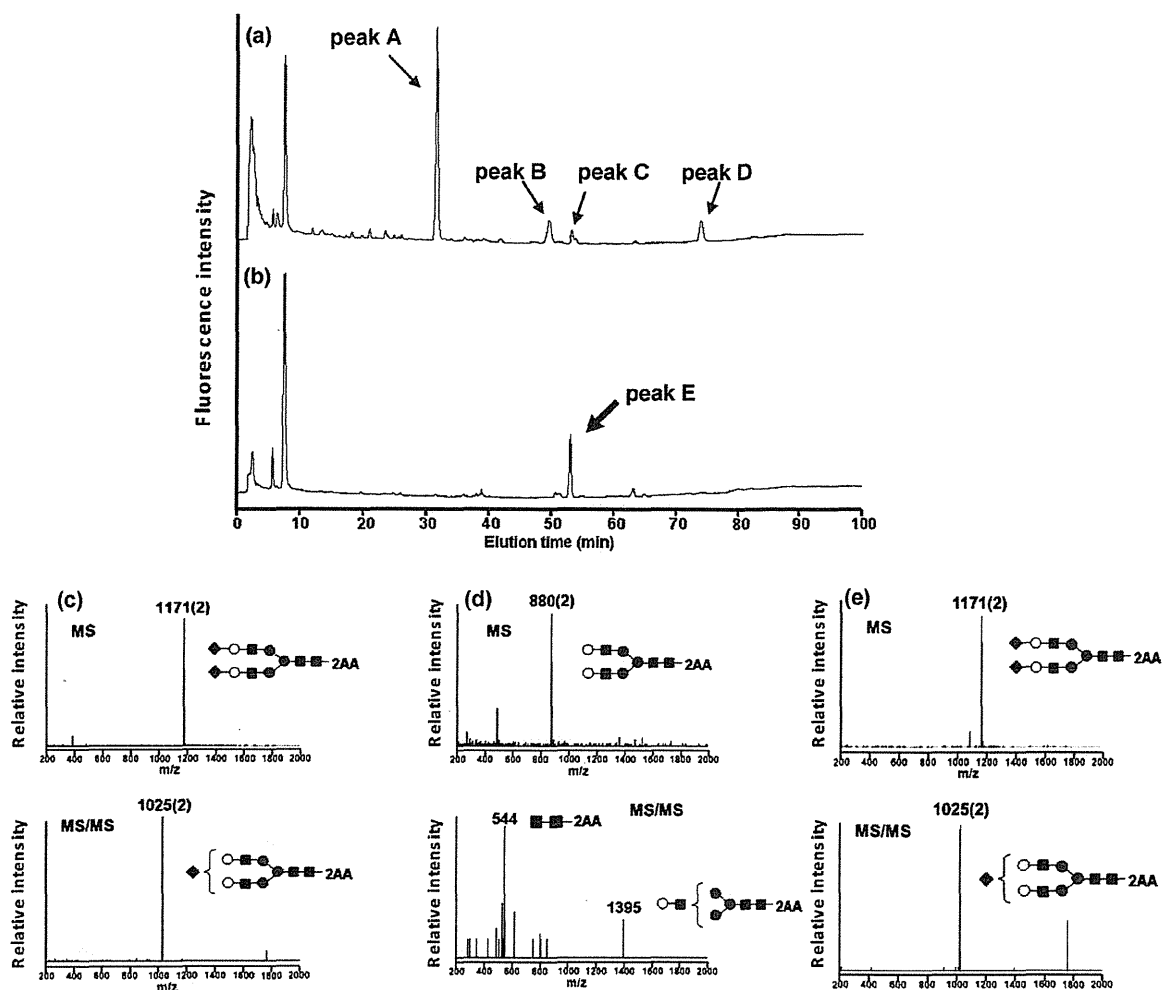


Fig. 1. HPLC Analysis of (a) mucin-type glycans from human serum released from the glycoproteins. (b) Intact serum sample after easy removal of low molecular weight materials. MS and MS/MS data of (c) peak C and (d) the product after neuraminidase digestion of peak C. (e) MS and MS/MS data of peak E. HPLC conditions: column, Asahi Shodex NH2P-50 4E(4.6 mm × 250 mm). Eluent solvent A, 2% acetic acid in acetonitrile, solvent B, 5% acetic acid, 3% triethylamine in water. Gradient condition: a linear gradient (30–95% solvent B) from 2 to 82 min, maintained for 20 min. Symbols: squares, N-acetylglucosamine; gray circles, mannose; white circles, galactose; diamonds, N-acetylneuraminic acid.

chemically released from the glycoproteins in a serum sample by an automatic manner developed by the authors [10–13], and analyzed by HPLC after labeling with a fluorescent reagent, 2AA. Four peaks (A–D) were detected at 30 (A), 46 (B), 53 (C) and 70 min (D), respectively. Peaks A, B and D were due to mucin-type O-glycans, and identified as sialyl T (NeuAc α 2-3Gal β 1-3GalNAc-2AA), degradation product (NeuAc α 2-3Gal) and disialyl T (NeuAc α 2-3Gal β 1-3[NeuAc α 2-6]GalNAc-2AA), respectively. A distinct peak (peak C) other than those of mucin-derived glycans was observed at 53 min. The MS and MS/MS spectra of the peak C are shown in Fig. 1c. The molecular ion of the peak was observed at m/z 1171 as a doubly charged ion, which was confirmed as disialo-biantennary glycan. And the ion due to monosialo biantennary glycan was observed in MS/MS spectra. The peak at 53 min was collected, and digested with neuraminidase. MS of the obtained asialoglycan showed the molecular ion at m/z 880 as a doubly charged ion (Fig. 1d). MS/MS spectra showed an ion due to chitobiosyl-2AA at m/z 544. These data clearly mean that peak C is due to disialobiantennary glycan. As indicated previously, the automatic apparatus employed for releasing O-glycans does not cleave Asn-GlcNAc linkage, and free N-glycans are not released from the protein core containing Asn-type glycoproteins [10]. This means

that glycan (due to peak C) was endogenously present in serum samples.

To demonstrate if the glycans are due to free glycans in sera, the glycans in sera were directly analyzed after labeling with 2AA. After removing the small-molecular weight materials including glucose and inorganic salts in sera by ultrafiltration and also removing hydrophobic materials using an ODS-cartridge, the eluate (equivalent to 2 μ L of sera) was analyzed by HPLC after labeling with 2-AA (Fig. 1b). A big peak (peak E) was observed at 53 min, which showed the same elution time with that of peak C observed in Fig. 1a. In addition, the peak showed the same MS and MS/MS profiles with those of peak C (Fig. 1e). In addition, the data also showed well matched results with those of biantennary glycan obtained from transferrin (data not shown). These results indicate that the peak at 53 min was clearly due to the glycan present in sera in free form. It should be noticed that some minor peaks were also observed from 25 min to 65 min.

3.2. Detailed analysis of free glycans in a serum sample

As described above, we found that free glycans are present in human serum samples. Fig. 2a shows the results on the detailed

Table 1
Summary of free glycans in human serum. (A) before neuraminidase digestion. (B) after neuraminidase digestion.

Peak no.	<i>m/z</i>	Monosaccharides composition	Content of free oligosaccharide (p mol/mL serum)
1	(A) 872 (2)	Hex ₄ dHex ₁ HexNAC ₄ -2AA	175
	(B) 872 (2)	Hex ₄ dHex ₁ HexNAC ₄ -2AA	
2	(A) 953 (2)	Hex ₅ dHex ₁ HexNAC ₄ -2AA	256
	(B) 953 (2)	Hex ₅ dHex ₁ HexNAC ₄ -2AA	
3, 4	(A) 794 (1)	NeuAc ₁ Hex ₁ HexNAC ₁ -2AA	264 (peak 3)
	(B) 503 (1)	Hex ₁ HexNAC ₁ -2AA	
5	(A) 1099 (2)	NeuAc ₁ Hex ₅ dHex ₁ HexNAC ₄ -2AA	235
	(B) 953 (2)	Hex ₅ dHex ₁ HexNAC ₄ -2AA	
6	(A) 1025 (2)	NeuAc ₁ Hex ₅ HexNAC ₄ -2AA	844
	(B) 880 (2)	Hex ₅ HexNAC ₄ -2AA	
7	(A) 1171 (2)	NeuAc ₂ Hex ₅ HexNAC ₄ -2AA	572
	(B) 880 (2)	Hex ₅ HexNAC ₄ -2AA	
8	(A) 1244 (2)	NeuAc ₂ Hex ₅ dHex ₁ HexNAC ₄ -2AA	642
	(B) 953 (2)	Hex ₅ dHex ₁ HexNAC ₄ -2AA	
9	(A) 1171 (2)	NeuAc ₂ Hex ₅ HexNAC ₄ -2AA	7620
	(B) 880 (2)	Hex ₅ HexNAC ₄ -2AA	
10	(A) 1070 (2)	NeuAc ₂ Hex ₅ HexNAC ₃ -2AA	235
	(B) 778 (2)	Hex ₅ HexNAC ₃ -2AA	
11-⊖	(A) 1048 (3)	NeuAc ₃ Hex ₆ dHex ₁ HexNAC ₅ -2AA	1206
	(B) 1136 (2)	Hex ₆ dHex ₁ HexNAC ₅ -2AA	
11-⊕	(A) 999 (3)	NeuAc ₃ Hex ₆ HexNAC ₅ -2AA	(Total contents for 11-⊖ and 11-⊕)
	(B) 1062 (2)	Hex ₆ HexNAC ₅ -2AA	

dHex, deoxyhexose; Hex, hexose; HexNAC, N-acetyl hexose; NeuAc, N-acetylneuraminic acid.

profile of free glycans present in a serum sample (equivalent to 100 μ L serum as the injected volume). Each peak was collected and their structures were confirmed by MS technique (Fig. 3 and Table 1). Most of the peaks are commonly found in transferrin and other commercially available samples, and their structures are easily confirmed. Disialylated biantennary glycan showing the molecular ion at *m/z* 1171 (peak 9) as the doubly charged ion was the most abundant glycan as already shown in Fig. 1. The amount was determined to be 7620 pmol/mL of serum as calculated from the fluorescent intensity based on 2-AA residue. Structures of the minor peaks were also determined by MS techniques and comparison of the elution times with those reported previously [9]. At the earlier elution times (ca. 25 min), neutral mono- and di-galactosylated biantennary glycans (1 and 2) were observed. Mono-sialylated biantennary glycans with or without a fucose residue were observed at ca. 39 min (5 and 6). In addition, trisialo-triantennary glycans with or without a fucose residue were also observed at 63 min (11). Interestingly, we found a glycan having a structure of NeuAc-Gal-GalNAC-2AA which is probably due to mucin-type glycoproteins, although the amount of these glycans were only ca. 250 pmol/mL of serum (3 and 4). These peaks (3 and 4) were also assigned by comparison of the elution times with

those reported previously [10]. A characteristic glycan (10), disialo-biantennary glycan having one GlcNAc residue at the reducing end was also present in sera. We previously reported that this glycan was characteristically accumulated in cytosols of stomach tumor cells. The presence of this glycan may indicate that this characteristic glycan is leaked from some organs, although further studies are required [9]. According to the MS observations, peak 7 was assigned as disialo biantennary glycan by MS measurement. This indicates that peak 7 has different linkages of NeuAc to Gal with those of peak 9. Because NeuAc mainly binds to Gal through α 2-6 linkage in human [20], the glycan (9) is a typical disialo biantennary glycan which has NeuAc α 2-6 linkages. And peak 7 is probably due to disialoglycan which has NeuAc α 2-3 linkages. We also analyzed total N-glycans in a serum sample in order to consider the origin of free glycans in serum in detail. Fig. 2b shows the results on the profile of total N-glycans present in a serum sample (equivalent to 0.75 μ L serum as the injected volume). As shown in Fig. 2b, the results are quite similar to those in Fig. 2a. It should be emphasized that high mannose-type glycans were not detected at all. This also indicates that these glycans are not due to cells from some organs but from sera, because high mannose-type glycans are major ones found in cytosol fractions through endoplasmic-reticulum associated protein degradation pathway [3].

Sturiale et al. studied glycosylation of transferrin in galactosemia patients in order to figure out hypoglycosylation with increased fucosylation and branching [21]. In the manuscript, they showed N-glycan profiles in a human serum sample (healthy volunteer) examined by MS technique after releasing N-glycans with N-glycoamidase F. The data showed quite similar profiles with those observed in the present study. Namely, Sturiale et al. reported that the ratios of triantennary glycan ((Fuc)Gal₃GlcNAc₅Man₃NeuAc₃), monosialo-biantennary glycan (Gal₂GlcNAc₄Man₃NeuAc) and disialo-fucosylated biantennary glycan (FucGal₂GlcNAc₄Man₃NeuAc₂) to the main glycan (Gal₂GlcNAc₄Man₃NeuAc₂) were 13.5, 9.4 and 6.5%, respectively. In the present study, the ratios of these glycans to the major glycan (9) were 15.8, 11.1 and 8.4%, respectively. These data clearly indicate that these glycans are possibly derived from serum glycoproteins containing transferrin during its circulation in bodies.

Free glycans found in the cytosol have only a single GlcNAc at their reducing termini [2], and this is due to the action of

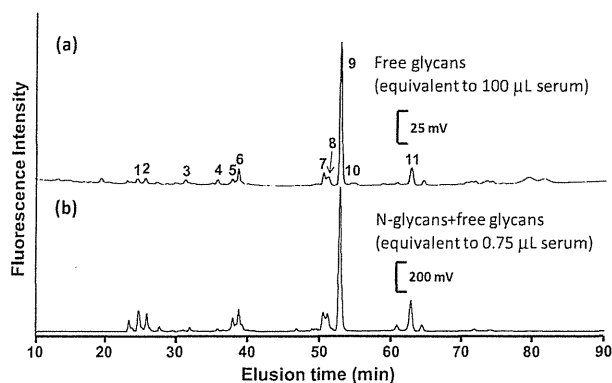


Fig. 2. HPLC analysis of (a) free glycans, and (b) total N-glycans in a human serum sample as examined after digestion with N-glycoamidase F. Analytical conditions are the same as those in Fig. 1.

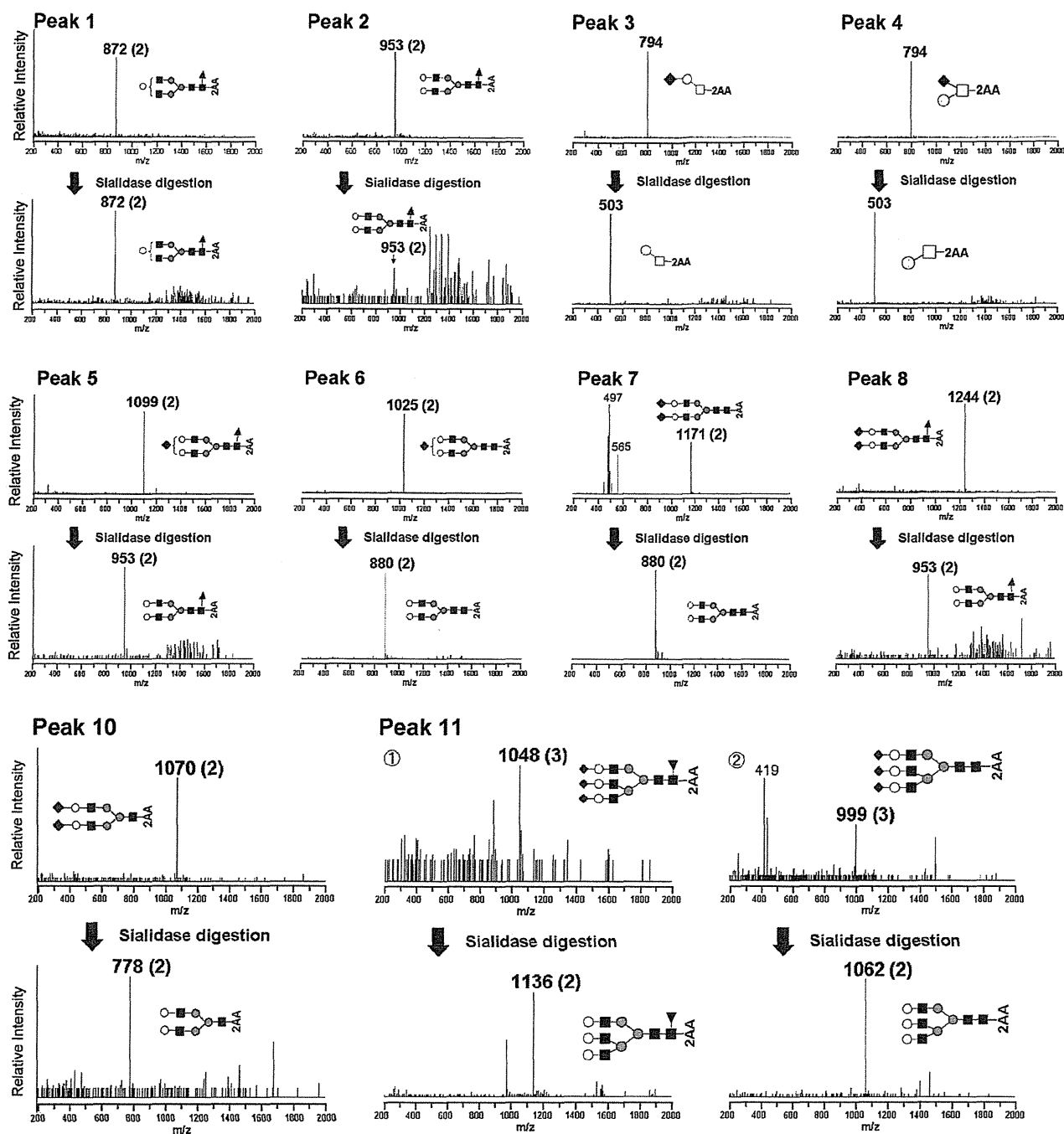


Fig. 3. ESI-IT-TOF mass spectra of peak 1–8, 10, 11 in Fig. 2. Symbols: triangles, fucose; others are the same as those in Fig. 1. Upper panels show the MS spectra of collected peaks. The collected peaks were digested with neuraminidase, and also analyzed by MS (lower panels).

the cytosolic ENGase (endo- β -N-acetylglucosaminidase) [22,23] or chitobiase [24]. It should be noted that most free glycans found in the present study bear N-acetylchitobiose structure other than peak **10**. Kimura et al. reported that free glycans were accumulated not only inside cells but also secreted to the extracellular space in rice cell culture [25,26]. In addition, they suggested that the extracellular acidic peptide N-glycanase was involved in accumulation of such glycans. We have to also consider the presence of free O-glycans (**3** and **4**), although the amounts of these glycans are quite small.

The mechanism of the presence/formation of free glycans in sera and the source of these glycans are not clear in the present study. However, it is quite interesting if these glycans are varied with physiological changes.

4. Conclusions

The present study demonstrates that free glycans exist in human serum. Most of the glycans were sialic acid-containing complex-type glycans. Of the glycans, disialo-biantennary glycan which does

not carry fucose residue is present most abundantly. And high mannose-type glycans were not detected at all. From these results, we suppose that these free glycans were due to glycoproteins in sera, although further studies are required.

References

- [1] D. Kmiecik, V. Herman, C.J. Stoop, A.M. Mir, O. Labiau, A. Verbert, *Glycobiology* 5 (1995) 483.
- [2] K. Yanagida, S. Natsuka, S. Hase, *Glycobiology* 16 (2006) 294.
- [3] T. Suzuki, H. Park, W.J. Lennarz, *FASEB J.* 16 (2002) 635.
- [4] I. Chantret, S.E. Moore, *Glycobiology* 18 (2008) 210.
- [5] T. Suzuki, Y. Funakoshi, *Glycoconj. J.* 23 (2006) 291.
- [6] D.J. Kelleher, R. Gilmore, *Glycobiology* 16 (2006) 47R.
- [7] T. Suzuki, *Semin Cell, Dev. Biol.* 18 (2007) 762.
- [8] R. Naka, S. Kamoda, A. Ishizuka, M. Kinoshita, K. Kakehi, *J. Proteome Res.* 5 (2006) 88.
- [9] A. Ishizuka, Y. Hashimoto, R. Naka, M. Kinoshita, K. Kakehi, J. Seino, *Biochem. J.* 413 (2008) 227.
- [10] Y. Matsuno, K. Yamada, A. Tanabe, M. Kinoshita, S. Maruyama, Y. Osaka, T. Masuko, K. Kakehi, *Anal. Biochem.* 362 (2007) 245.
- [11] K. Yamada, S. Hyodo, Y. Matsuno, M. Kinoshita, S. Maruyama, Y. Osaka, E. Casal, Y.C. Lee, K. Kakehi, *Anal. Biochem.* 371 (2007) 52.
- [12] K. Yamada, M. Kinoshita, T. Hayakawa, S. Nakaya, K. Kakehi, *J. Proteome Res.* 8 (2009) 521.
- [13] K. Yamada, S. Hyodo, M. Kinoshita, T. Hayakawa, K. Kakehi, *Anal. Chem.* 82 (2010) 7436.
- [14] B. Winchester, *Glycobiology* 15 (2005) 1R.
- [15] J.C. Michalski, J. Lemone, J.M. Wieruszkeski, B. Fournet, J. Montreuil, G. Strecker, *Eur. J. Biochem.* 198 (1991) 521.
- [16] G. Strecker, M.C. Peers, J.C. Michalski, T. Hondi-Assah, B. Fournet, G. Spik, J. Montreuil, J.P. Farriaux, P. Maroteaux, P. Durand, *Eur. J. Biochem.* 75 (1977) 391.
- [17] J. van Pelt, K. Hard, J.P. Kamerling, J.F. Vliegthart, A.J. Reuser, H. Galjaard, *Biol. Chem. Hoppe-Seyler* 370 (1989) 191.
- [18] K. Ishii, M. Iwasaki, S. Inoue, P.T.M. Kenny, H. Komura, Y. Inoue, *J. Biol. Chem.* 264 (1989) 1623.
- [19] M. Tajiri, C. Ohyama, Y. Wada, *Glycobiology* 18 (2008) 2.
- [20] G. Weisshaar, J. Hiyama, A.G.C. Renwick, *Glycobiology* 1 (1991) 393.
- [21] L. Sturiale, R. Barone, A. Fiumara, M. Perez, M. Zaffanello, G. Sorge, L. Pavone, S. Tortorelli, J.F. O'Brien, J. Jaeken, D. Garozzo, *Glycobiology* 15 (2005) 1268.
- [22] T. Kato, K. Hatanaka, T. Mega, S. Hase, *J. Biochem.* 122 (1997) 1167.
- [23] T. Suzuki, K. Yano, S. Sugimoto, K. Kitajima, W.J. Lennarz, S. Inoue, Y. Inoue, Y. Emori, *Proc. Natl. Acad. Sci. U.S.A.* 99 (2002) 9691.
- [24] R. Cacan, C. Dengremont, O. Labiau, D. Kmiecik, A. Mir, A.M. Verbert, *J. Biochem.* 313 (1996) 597.
- [25] Y. Kimura, S. Matsuo, *J. Biochem.* 127 (2000) 1013.
- [26] M. Maeda, M. Kimura, Y. Kimura, *J. Biochem.* 148 (2010) 681.

Masahiro Yodoshi
Natsumi Ikeda
Naoko Yamaguchi
Mana Nagata
Noriaki Nishida
Kazuaki Kakehi
Takao Hayakawa
Shigeo Suzuki

Faculty of Pharmaceutical
Sciences, Kinki University,
Kowakae, Higashi-Osaka, Osaka,
Japan

Received November 13, 2012
Revised September 2, 2013
Accepted September 5, 2013

Research Article

A novel condition for capillary electrophoretic analysis of reductively aminated saccharides without removal of excess reagents

We have identified novel CE conditions for the separation of 7-amino-4-methylcoumarin-labeled monosaccharides and oligosaccharides from glycoproteins. Using a neutrally coated capillary and alkaline borate buffer containing hydroxypropylcellulose and ACN, saccharide derivatives form anionic borate complexes, which move from the cathode to the anode in an electric field and are detected near the anodic end. Excess labeling reagents and other fluorescent products remain at the cathodic end. Fluorimetric detection using an LED as a light source enables determination of monosaccharide derivatives with good linearity between at least 0.4 and 400 μM , may correspond to 140 amol to 140 fmol. The lower LOD ($S/N = 5$) is only 80 nM in the sample solution (ca. 28 amol). The results were comparable to reported values using fluorometric detection LC. The method was also applied to the analysis of oligosaccharides that were enzymatically released from glycoproteins. Fine resolution enables profiling of glycans in glycoproteins. The applicability of the method was examined by applying it to other derivatives labeled with nonacidic tags such as ethyl *p*-aminobenzoate- and 2-aminoacridone-labeled saccharides.

Keywords:

7-Amino-4-methylcoumarin / Borate complex / Glycoprotein glycans / Monosaccharide analysis / Reductive amination
DOI 10.1002/elps.201200612

1 Introduction

Most saccharides are neutral, highly hydrophilic, and do not possess chromophoric or fluorometric functions. Various labeling reagents have therefore been developed to improve sensitivity and enhance resolution in LC and CE. Numerous fluorescent amines have been reported for the derivatization of saccharides based on reductive amination. In this labeling reaction, a saccharide is converted to a Schiff's base in the presence of a large excess of an aromatic amine and the resultant imide derivative is converted immediately to a chemically stable 1-amino-1-alditol by reduction with sodium cyanoborohydride. These reactions are well summarized in a number of reviews [1–3]. 8-Aminopyrene-1,3,6-trisulfonic

acid (APTS) is often used for sensitive detection of glycoprotein glycans in CE analysis because APTS derivatives show intense fluorescence signals under irradiation by an argon ion laser. The negative charge attributable to the three sulfonate groups of APTS moves derivatized saccharides to the anode at high velocity, which enables the rapid analysis of glycoprotein glycans [4–8]. 2-Aminopyridine is often used for identification of glycoprotein-derived oligosaccharides because retention indices for more than several hundred glycans have been accumulated in RP and normal phase LC, as well as anion-exchange LC for sialylated oligosaccharides [9–13]. However, the high hydrophilicity of APTS and 2-aminopyridine hampers solvent extraction of excess reagents. Therefore, tedious steps are required to remove excess reagents from the reaction mixture. Moreover this process may cause partial loss of derivatives, which impairs quantitative analysis.

We previously described a labeling method using 7-amino-4-methylcoumarin (AMC) as a fluorescent probe [14]. AMC-labeled oligosaccharides displayed one- to two-order higher intensities in ESI-MS than derivatives labeled with other reagents. However the method requires two-step SPE for the removal of excess AMC and by-products generated in the course of reaction, which requires tedious procedures and may partially impair quantitative determination.

Correspondence: Dr. Shigeo Suzuki, Faculty of Pharmaceutical Sciences, Kinki University in 3-4-1, Kowakae, Higashi-Osaka, Osaka, Japan

E-mail: suzuki@phar.kindai.ac.jp

Fax: +81-6-6721-2353

Abbreviations: ABEE, ethyl *p*-aminobenzoate; AMAC, 2-aminoacridone; AMC, 7-amino-4-methylcoumarin; APTS, 8-aminopyrene-1,3,6-trisulfonic acid; BSM, bovine submaxillary mucin; Fuc, fucose; Gal, galactose; GalNAc, *N*-acetylgalactosamine; GlcNAc, *N*-acetylglucosamine; IS, internal standard; Man, mannose; ManNAc, *N*-acetylmannosamine; NeuAc, *N*-acetylneuraminic acid; NeuGc, *N*-glycolylneuraminic acid; Rha, rhamnose; Xyl, xylose

Colour Online: See the article online to view Fig. 5 in colour.

This work presents selective and sensitive separation conditions for profiling monosaccharides and oligosaccharides found in glycoproteins, without requiring the two-step extractive removal of excess labeling reagent. AMC-labeled saccharides have no charge in alkaline buffer. However in the presence of boric acid, the adjacent hydroxyl groups on saccharides form acidic complexes with borate, which provide a strong negative charge to AMC-labeled saccharides and induces their movement toward the anode. This method allows selective quantification of all of component monosaccharides found in glycoprotein hydrolysates; *N*-acetylglucosamine (GlcNAc), *N*-acetylgalactosamine (GalNAc), galactose (Gal), mannose (Man), fucose (Fuc), *N*-acetylneuraminic acid (NeuAc), and *N*-glycolylneuraminic acid (NeuGc). Application of LED-based fluorescent detection enables subattomole level detection of monosaccharides. This borate-based separation mode was also applied to the selective detection of glycoprotein-derived oligosaccharides.

2 Materials and methods

2.1 Materials

We obtained AMC from Tokyo Kasei Kogyo Co. (Tokyo, Japan). Pyridine-borane, DMF, ethyl *p*-aminobenzoate (ABEE), ACN, methanol, TFA, and glacial acetic acid were obtained from Wako Pure Chemical Industries (Doshomachi, Osaka, Japan). β -*N*-Acetylhexosaminidase (jack bean, EC 3.2.1.52) and β -galactosidase (jack bean, EC 3.2.1.23) were obtained from Seikagaku Kogyo K.K. (Tokyo, Japan). Dimethylamine-borane complex, 2-aminoacridone (AMAC), *N*-acetylneuraminidase pyruvate-lyase from *Escherichia coli* K-12, human transferrin, fetal calf serum fetuin, bovine pancreas ribonuclease B, human α_1 -acid glycoprotein, bovine submaxillary mucin (BSM), and ovalbumin were obtained from Sigma-Aldrich Japan K.K. (Tokyo, Japan). Neuraminidase from *Arthrobacter ureafaciens* and saccharide specimens were obtained from Nacalai Tesque (Kyoto, Japan). Peptide-*N*^t-(acetyl- β -glucosaminyl)-asparagine amidase F (EC 3.5.1.52) was purchased from F. Hoffmann-La Roche (Mannheim, Germany). Isomaltooligosaccharides were obtained through partial hydrolysis of dextran (100 mg) with 1 mL of 0.1 M hydrochloric acid for 4 h at 100°C; the lyophilized powder was used as a glucose ladder. Water was purified using a Milli-Q device (Millipore, Milford, MA, USA). Other reagents and solvents were of the highest commercially available grade. In addition, SCX-type SPE cartridges (100 mg) and OASIS HLB cartridges (10 mg) were obtained from Silicycle (Quebec, Canada) and Nihon Waters K.K. (Tokyo, Japan), respectively. Graphitized carbon was from Alltech Japan (Tokyo, Japan). AMC-labeled maltose was prepared as described in a previous report, and AMC-labeled oligosaccharides derived from glycoprotein specimens were fractionated by HPLC and used for peak identifications [14].

2.2 Hydrolysis of glycoprotein specimens

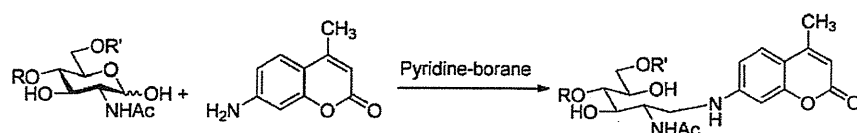
Hydrolysis of glycoprotein specimens was carried out as previously described [15]. Two portions of a solution of glycoprotein specimen (0.1 mg each) were lyophilized in glass tubes (4 mm id, 12 cm long). For the analysis of component neutral aldoses, one of the sample residues was dissolved in 100 μ L of 2 M TFA and the tube was sealed after exchanging air in the tube with nitrogen three times using a vacuum desiccator connected to nitrogen and vacuum lines, and the tube was then sealed and heated for 6 h at 100°C. The resultant solution was mixed with 20 μ L of 0.1 mM rhamnose (Rha, 2 nmol) as internal standard (IS), and the residue was lyophilized to dryness for derivatization with AMC. For the analysis of hexosamines, a sample was dissolved in 100 μ L of 4 M HCl and the solution was heated for 6 h at 100°C under a nitrogen atmosphere. The solution was then evaporated to dryness, followed by addition of 2 nmol IS. Acetamide groups were hydrolyzed in this process. Therefore the residue was dissolved in 250 μ L of a saturated solution of sodium bicarbonate and the solution mixed with 50 μ L of acetic anhydride under vigorous shaking for 30 min and stored in a refrigerator overnight. The reaction mixture was mixed with 500 μ L of water and DI by passing through a column containing 1 mL of Amberlite CG120 (H⁺ form) resin, and the column was then washed with 5 mL of water. The combined eluate and washing fluids were evaporated to dryness and derivatized with AMC. For the analysis of sialic acids, a glycoprotein sample was dissolved in 100 μ L of 60 mM phosphate buffer (pH 7.0) containing neuraminidase (0.1 U) and *N*-acetylneuraminidase pyruvate-lyase (0.1 U), and the mixture was incubated for 5 h at 37°C. After the mixture was heated for 1 min at 100°C, the solution was DI with a column containing 1 mL each of Amberlite CG120 (H⁺ form) and CG400 (acetate form) resins, followed by addition of 2 nmol IS.

2.3 Preparation of oligosaccharides from glycoproteins

N-Linked oligosaccharides were prepared from 50 μ g of each lyophilized glycoprotein. Each sample was dissolved in 50 μ L of 50 mM phosphate buffer (pH 7.9) containing 0.1% SDS and 2% 2-mercaptoethanol. The solution was heated at 100°C for 5 min. After cooling, the solution was mixed with 5 μ L of 7.5% NP-40 and 5 mU of peptide-*N*^t-(acetyl- β -glucosaminyl)-asparagine amidase F, and the reaction mixture incubated for 2 h at 37°C. Deglycosylated proteins were precipitated by the addition of 180 μ L of ice-cold ethanol and removed by centrifugation at 10 000 rpm for 5 min. The supernatant was dried using a centrifugal evaporator (Tomy, Tokyo, Japan) and stored in a refrigerator until use.

2.4 Derivatization of saccharides with AMC

Scheme 1 shows the reductive amination reaction of saccharides with AMC. The procedure was described previously [14].



Scheme 1. Reductive amination of a saccharide with AMC as a fluorescent tag.

Briefly, a lyophilized sample containing saccharides (~10 nmol) in a screw-capped polypropylene tube (0.5 mL volume) was mixed with 20 μ L of AMC solution (60 mM in DMF) and then mixed with 20 μ L of pyridine–borane solution (0.2 M in acetic acid). The solution was then heated at 70°C for 60 min and the reaction terminated by addition of 60 μ L of water and chilling of the reaction mixture in an ice bath, followed by evaporation to dryness. The resultant residues were dissolved in 500 μ L of 0.5 M acetic acid in aqueous 30% ACN for CE analysis.

2.5 Derivatization of saccharides with AMAC and ABEE

A monosaccharide mixture or isomaltooligosaccharides was labeled according to previously reported methods [16, 17] with slight modification. Each 2.5 μ L of 0.3 M AMAC in DMSO/30% acetic acid (7:3, v/v), and 1 M NaBH₃CN in DMSO was added to dry saccharide samples (~10 nmol). The solution was incubated at 37°C overnight and the reaction terminated by adding 50 μ L of water–methanol (1:1, v/v).

A 20 μ L portion of ABEE solution (1 mmol of ABEE and 35 mg of NaBH₃CN, and 41 μ L of acetic acid dissolved in 350 μ L of methanol) was added to a saccharide sample (~100 nmole), and the solution was heated at 80°C for 1 h. The resultant solution was dried and dissolved in 100 μ L of water–methanol (9:1, v/v). Excess ABEE, immiscible in the solvent, was removed by centrifugation, and the supernatant was used for the CE analysis.

2.6 Instrumentation for CE analysis

Apart from a reference experiment using a bare fused silica capillary (50 μ m id) for Fig. 1A, PDMS-coated capillaries (InertCap I®; GL Sciences, Tokyo, Japan) of 50 μ m id with an effective length of 40 cm (50 cm in total) were used, with a 1:9, v/v, mixture of ACN and borate buffer containing 0.05% hydroxypropylcellulose as a BGE; 200 mM sodium borate (pH 9.5) for monosaccharide analysis and 250 mM potassium borate (pH 9.0), and 100 mM Tris borate (pH 8.5) for neutral and acidic oligosaccharide separation, respectively. A P/ACE MDQ CE system (Beckman Coulter, Brea, CA, USA) was used. An LED light (LLS-365, Ocean Photonics) as a source of 365 nm light was connected with an optical fiber (P600-2-UV/Vis, Ocean Photonics), and the fluorescence due to AMC derivatives was detected by passing through a 420 nm band path filter. The capillary was thermostated at 25°C. Sample

solution was injected for 5 s by application of pressure of 3.45 kPa. Separation was conducted by application of –15 kV. After each run, the capillary was washed by introducing a buffer solution from the outlet of the capillary using pressure (34.5 kPa, 2 min). AMAC derivatives were detected fluorometrically using an argon laser (488 nm) and the optical system for the fluorescein detection. ABEE derivatives were detected based on absorbance at 312 nm. Other conditions were the same as those for AMC derivatives.

The volume of sample solution injected into the capillary was not certain. Here we chose the following calculation to estimate injected amount of sample in sample solution:

$$V = \frac{\Delta P d^4 \pi t}{128 \eta L}$$

where V is the volume in m³ delivered across the capillary, ΔP denotes the pressure drop across the capillary (Pa), d signifies the internal diameter of the capillary (m), t is the duration of pressure application (s), η represents the buffer viscosity (Pa·s), and L is the total capillary length (m).

3 Results and discussion

3.1 Optimization of separation conditions

Alkaline borate buffer has often been used in CE separation of mixtures of monosaccharide derivatives [18]. Borate forms complexes with polyalcohols, including saccharide derivatives in solution, and the borate–polyalcohol complexes possess negative charges, which are forced to move toward the anode in an electric field. Stability and negativity of the saccharide–borate complex depend on the configuration of adjacent hydroxyl groups (i.e., the type of monosaccharide). Moreover, the pH and concentration of borate buffer influence the formation of polyoxy acid with borate ions as well as the complex formation, and therefore also affect the mobility of borate–polyol complexes [19]. Most reports on CE of monosaccharide derivatives using alkaline borate buffer were performed using a bare fused silica capillary. Under such conditions, monosaccharide derivatives travel from anode to cathode because of strong EOF, and separate as anions, based on the molecular size and stability of the borate complexes. Moreover, a large amount of excess fluorescent reagents also travels to the cathode, which may cause deviations in migration times and heavy drift of baselines.

Here, we used a PDMS-coated capillary instead of a bare fused silica capillary to suppress EOF and to specifically move acidic borate–saccharide complexes toward the anode. Reductive amination of carbohydrates with primary amines generates secondary amine derivatives of linear polyalcohols (i.e.,

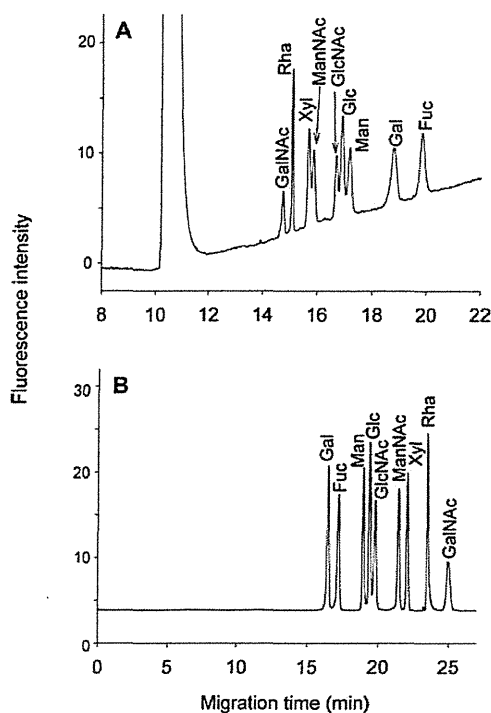


Figure 1. Fluorescent CE analysis of selected monosaccharides in borate complexation mode using a bare fused silica capillary (A) and a PDMS-coated capillary (B). Analytical conditions: BGE, ACN and 200 mM sodium borate (pH 9.5) containing 0.05% hydroxypropylcellulose (1:9, v/v); capillary size, 50 μm id \times 50 cm (40 cm for detector); capillary temperature, 25°C; applied voltage +15 kV (A) and -15 kV (B); detection, fluorescence with 365 nm LED.

aminoalditols). Excess aromatic amines and their decomposition products residing in the reaction mixture cannot be charged in alkaline borate buffer. In contrast, monosaccharide derivatives having linear polyalcohol structures easily generate negative charges as borate complexes, which move toward the anode in an electric field. Therefore, the excess reagents in the reaction mixture can be removed from electropherograms without requiring purification before analysis.

Figure 1A shows the separation of AMC derivatives of monosaccharides obtained by reaction on positive mode separation using a bare capillary and alkaline borate buffer as BGE. Reaction products of AMC-labeled derivatives show an intense, tailing signal of excess AMC at 11 min and baseline drift, which could not be removed by addition of surfactants to the BGEs. In contrast, a combination of negative separation mode using 200 mM borate buffer containing 0.05% hydroxypropylcellulose and PDMS-coated capillary, as shown in Fig. 1B, suppressed the generation of EOF and therefore induced the movement of anionic borate complexes to the anode. This enables specific detection of saccharide derivatives. Addition of ACN prevents the precipitation of excess reagent. Therefore, the electropherogram comprised peaks corresponding to monosaccharide derivatives, with no peaks

because of excess reagent. This result indicates the usefulness of the separation conditions.

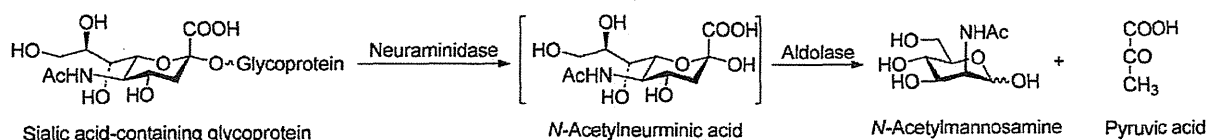
3.2 Monosaccharide analysis

We previously reported that the use of pyridine-borane rather than the sodium cyanoborohydride normally used enables quantitative derivatization of all component monosaccharides in glycoproteins [14]. Here, we optimized the separation conditions of AMC-labeled monosaccharides containing excess reagents using CE with fluorometric detection by LED.

The resolution between AMC monosaccharide derivatives depends strongly on the pH of the borate buffer and also the species and concentration of organic solvent. Resolution of Man-Glc-GlcNAc and ManNAc-Xyl is invariant with pH but the separation window (i.e., time window for separation of monosaccharides) is broadened with increasing electrophoresis buffer pH. The concentration of the borate buffer mainly affects the peak shape of AMC derivatives. With increasing buffer concentration, the sharpness of AMC monosaccharide peaks increased, reaching a maximum of over 200 mM. The higher concentration causes Joule heating because of the increase in electric current. Addition of a water-miscible solvent such as methanol, ethanol, or ACN is essential to prepare a clear solution from the AMC reaction mixture because of the low solubility of AMC in water. Among these three solvents, we found that the addition of ACN enhanced the resolution of fucose from other monosaccharide derivatives. Baseline resolution was obtained using a 1:9 v/v mixture of ACN and borate buffer containing 0.05% hydroxypropylcellulose. However, the anions residing in the reaction mixture partly diminished the sharpness of specific peaks. To enhance the sharpness of saccharide peaks, acetic acid was added to AMC-labeled sample at a concentration of 0.5 M. Good resolution between the nine monosaccharide derivatives was obtained under the optimized conditions, as shown in Fig. 1B.

3.3 Analysis of component monosaccharides in glycoproteins

The optimized conditions were applied to the analysis of component monosaccharides in a number of glycoproteins. Saccharide chains in glycoproteins comprise Man, Gal, Fuc, GlcNAc, GalNAc, NeuAc, and NeuGc. Before the analysis, the linearity range and lower LOD were examined. As shown in Fig. 2, linear quantitation ranges were obtained over the concentration range between at least 0.4 and 400 μM (calculated to be 140 amol to 140 fmol). Figure 3 shows the separation of 4, 0.4, and 0.04 μM mixture. Apparently, 4 and 0.4 μM are within the quantitation range, but the concentration of 0.04 μM were apparently below the detection limit, for example, peak height of Rha is only 2.5 times of noise. Therefore we determined 80 nM (ca. 28 amol) as the LOD ($S/N = 5$). The hydrolytic conditions required for quantitative



Scheme 2. Enzymatic conversion of sialic acids in glycoproteins to mannosamine derivatives.

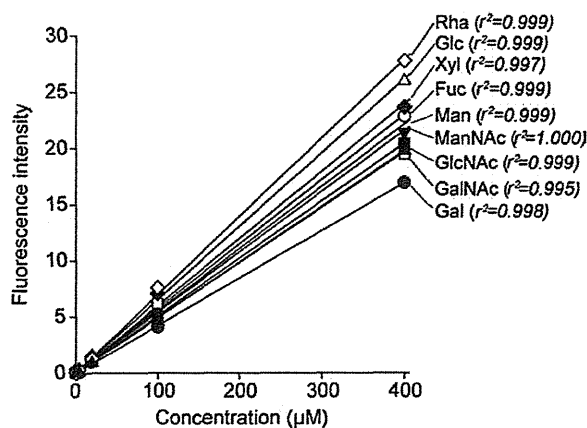


Figure 2. Calibration plots for quantitation of nine saccharides as AMC derivatives.

recovery of monosaccharides vary depending on the type of monosaccharides [20]. Therefore, we used different conditions for neutral aldoses, hexosamines, and sialic acids. Two molar TFA was chosen for hydrolysis of neutral aldoses, including Fuc, Gal, and Man, while 4 M hydrochloric acid was used for the release of hexosamines. Hydrolysis was performed at 100°C for 6 h. In contrast sialic acids are easily decomposed in strong acids so we chose enzymatic release and the generated neuraminic acids were further converted to *N*-acetyl- or *N*-glycolylmannosamine derivatives by the action of aldolase (*N*-acetylneuraminic acid pyruvate-lyase, EC 4.1.3.3), as shown in Scheme 2 [15]. Therefore, the contents of both types of neuraminic acid could be estimated from the peak areas of corresponding mannosamine derivatives, appearing at 17.5 and 18.5 min, respectively.

Figure 4 indicates the results of monosaccharide analysis of several glycoprotein samples. Rha was chosen as a common IS for the analysis. Acid glycoprotein, fetuin, ovalbumin,

ribonuclease B, and transferrin were chosen as common glycoproteins, and BSM was used for sialic acid analysis because mucin contains high concentrations of NeuAc and NeuGc. Carbohydrate chains of acid glycoprotein and transferrin are composed of complex oligosaccharides, whose chains consist of GlcNAc, Man, Gal, Fuc, and NeuAc [21, 22]. Electropherograms clearly indicated the presence of these monosaccharides. The fucose content of transferrin is low but the electropherogram clearly indicated the presence of Fuc in the hydrolysates of transferrin. Fetuin contains both *N*- and *O*-linked glycans [23–25]. Therefore, the oligosaccharide chains are composed of GlcNAc, GalNAc, Man, Gal, and neuraminic acids. These monosaccharides appeared in the electropherograms. Moreover, a small peak of *N*-glycolylmannosamine indicates the presence of NeuGc in this glycoprotein, at a level one order lower than that of NeuAc. Ovalbumin comprises high-mannose type and a series of hybrid-type glycans, which implies the presence of GlcNAc, Man, and a small quantity of Gal [26–28]. RNB comprises a series of high-mannose type oligosaccharides [29]. Therefore, hydrolysates include only Man and GlcNAc. These monosaccharides appeared in electropherograms.

Based on the peak area of each sample relative to IS, the monosaccharide contents were estimated and are summarized in Table 1. The results were compared to those of previously reported data [15, 30]. The accuracy of the present method involving the hydrolysis process could not be fully evaluated by comparison with previous data as contents of fucose in acid glycoprotein, Man in fetuin, and GlcNAc and neuraminic acids in transferrin were apparently lower than the reported values. In contrast, Man in ribonuclease and hexosamines in fetuin were at higher levels than previously reported. The sialic acid contents of BSM were three times higher than those of reported values, which should be due to difference in commercial preparation. We believe the removal of the purification step for derivatives could enhance the

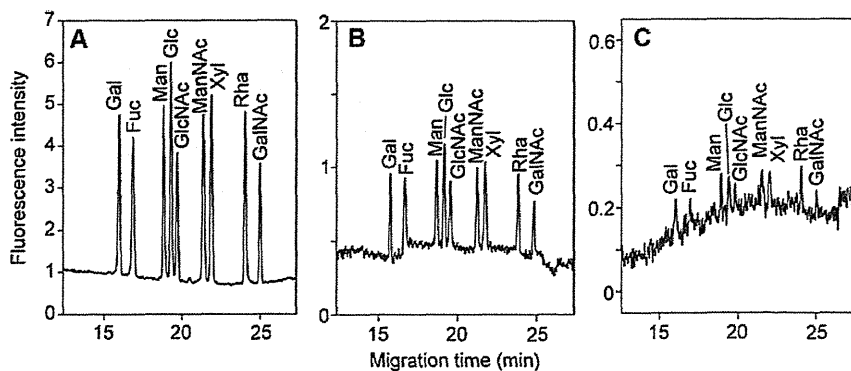


Figure 3. CE analysis of nine saccharides at concentrations of 4 μM (A), 0.4 μM (B), and 0.04 μM (C). Analytical conditions were the same as those used for Fig. 1B.

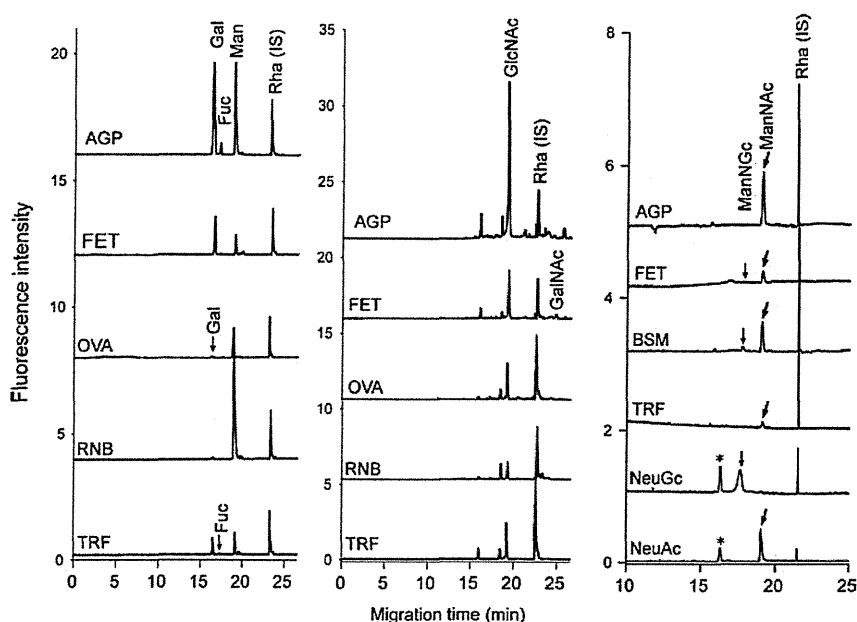


Figure 4. Analysis of component monosaccharides in hydrolysates of various glycoproteins. Analytical conditions were the same as those used for Fig. 1B. ManNGc and ManNAc were derived from NeuGc and NeuAc, respectively. AGP = α_1 -acid glycoprotein, FET = fetuin, OVA = ovalbumin, RNB = ribonuclease B, TRF = transferrin.

Table 1. Estimated content (%) of monosaccharides in various glycoprotein specimens

Glycoprotein	Man ^{a)}	Gal ^{a)}	GlcNAc ^{a)}	GalNAc ^{a)}	NeuAc ^{b)}	NeuGc ^{b)}	Fuc ^{a)}
α_1 -Acid glycoprotein (human)	5.80	8.99	13.88	N.D.	10.02	N.D.	0.47
	5.50	7.60	13.20	N.D.	10.90	N.D.	0.70
Fetuin (bovine)	1.60	3.15	4.26	1.30	6.28	0.68	0.04
	2.45	3.49	2.62	0.54	4.62	–	0.03
Transferrin (human)	1.15	0.76	1.27	N.D.	0.91	N.D.	0.07
	1.08	1.00	1.79	0.05	1.40	N.D.	–
Submaxillary mucin (bovine)	–	–	–	–	5.80	4.59	–
	–	–	–	–	1.69	1.25	–
Ovalbumin (hen)	2.47	0.11	1.63	N.D.	N.D.	N.D.	N.D.
	2.80	0.12	0.28	N.D.	N.D.	N.D.	N.D.
Ribonuclease B (bovine)	4.63	N.D.	1.09	N.D.	N.D.	N.D.	N.D.
	2.20	N.D.	0.91	N.D.	N.D.	N.D.	N.D.

Values appearing on the lower line for each glycoprotein indicate reference values. N.D.: not detected; –: not determined.

a) Ref. [30].

b) Ref. [15].

reliability of quantitation for saccharides in glycoconjugate samples. Our data may therefore be more reliable than that from previously reported methods and, moreover, the sensitivity is far superior to previous methods.

3.4 Analysis of oligosaccharides in glycoproteins

The resolution of AMC-labeled oligosaccharides was evaluated using a series of α 1,6-linked glucose oligomers called isomaltooligosaccharides, which had DPs distributed from 1 to 20 or more. Boric acid forms a stable complex with the linear polyalcohol structure at linear monosaccharide residues linked to AMC and the binding ability of borate to ring-formed monosaccharide residues is not high. They migrated in the

order of increasing DP because of the low mobility of oligosaccharides due to the low binding capability to borate ions. To enhance the apparent mobility of AMC-oligosaccharides, we chose 250 mM potassium borate buffer (pH 9.0). As shown in Fig. 5A, they were completely resolved and oligosaccharides corresponding to DPs of more than 20 were detected within 60 min. Most N-linked oligosaccharides in glycoproteins are distributed between DPs of 7 and 20, which indicate that it is possible to separate a neutral oligosaccharide mixture of glycoproteins by this mode.

The separation conditions were applied to the analysis of AMC-labeled N-linked oligosaccharides from transferrin, fetuin, and ribonuclease B. However, the separation of acidic oligosaccharides derived from transferrin and fetuin indicates finer resolution using a somewhat lower pH of borate

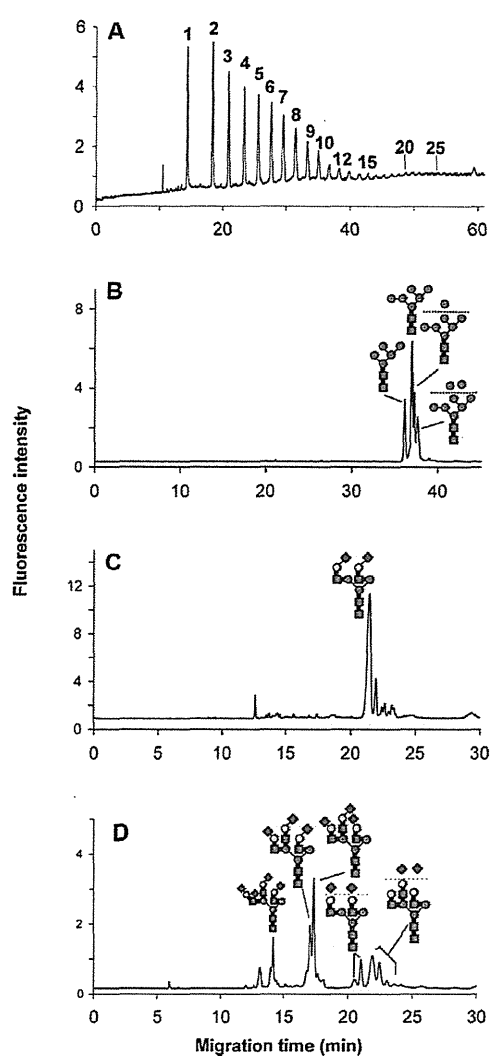


Figure 5. Separation of a mixture of isomaltooligosaccharides (A), ribonuclease B (B), transferrin (C), and fetuin (D). BGE, 1:9, v/v, mixture of ACN and borate buffer containing 0.5% hydroxypropylcellulose; 250 mM potassium borate (pH 9.0) for (A) and (B), and 100 mM Tris borate (pH 8.5) for (C) and (D), respectively.

buffer. Therefore, we applied 100 mM Tris borate (pH 8.5) for acidic oligosaccharide separation and 250 mM potassium borate buffer (pH 9.0) for neutral oligosaccharides. Results are shown in Fig. 5B–D. Oligosaccharide structures in each peak indicate there was identification based on co-migration of an AMC-oligosaccharide pool prepared by HPLC fractionation [14].

RNB contains a series of high-mannose type oligosaccharides. Their separation profile (Fig. 5B) indicates they migrated in order of their size, Man₅ to Man₉. However the separation mode could not separate linkage isomers of Man₇ and Man₈ high-mannose type oligosaccharides.

Oligosaccharides of transferrin (Fig. 5C) are mainly composed from disialylated biantennary oligosaccharides, which appeared as a large peak at 20.5 min. The subsequent small

peaks should be assigned to fucosylated biantennary oligosaccharides.

Fetuin mainly contains a series of di-, tri-, and tetra-sialylated triantennary glycans with variation in the linkage isomers of neuraminic acids and the presence of the Lewis X-type branch in the α 1,4-linked Gal–GlcNAc branch. As shown in Fig. 5D, AMC oligosaccharides from fetuin were mainly separated according to the number of sialic acids and were further resolved by the linkage type and position as well as differences in the lactosamine linkage. The peaks detected at 14, 17, and 20–22 min correspond to tetra-, tri-, and di-sialylated oligosaccharides. Furthermore, four peaks appearing at 20–22 min correspond to biantennary and triantennary di-sialylated oligosaccharides. Di-sialylated triantennary oligosaccharides may be generated from partial loss of a sialic acid from triantennary oligosaccharides, which causes numerous linkage isomers and appeared as a broad peak at 22 min. Unfortunately, this separation mode is not suitable for the resolution of these oligosaccharide isomers.

3.5 Application to the separation of saccharides using other labels

Finally, as a practical test, monosaccharide mixtures and isomaltooligosaccharides were labeled with AMAC and ABEE, and the derivatives were subjected to separation with borate complex mode CE, as shown in Figs. 5A and 1B, respectively. As shown in Fig. 6, AMAC- and ABEE-labeled saccharides showed an essentially identical pattern to AMC saccharides and were also free from interference by excess reagents. ABEE derivatives migrated faster than those of AMAC derivatives so the resolution of AMAC-oligosaccharides was high. The resolution of the Glc and GlcNAc pair was achieved using ABEE derivatives. We also evaluated these separation conditions for other labels, such as *p*-aminobenzonitrile (ABN) and 5-amino-1-naphthol (AN). However, the reaction products of isomaltooligosaccharides and ABN showed an intense, unknown signal at ca. 5 min, and that of AN showed an unknown peak at 15 min (data not shown). We speculate that these peaks may be due to the products of degradation of reagents, generated during derivatization reactions.

4 Concluding remarks

A combination of alkaline borate buffer and a neutrally coated capillary enables specific determination of AMC-labeled oligosaccharides, and an LED-based fluorimetric detection was applied to sub-amol level detection of saccharides. This method enables analysis without removal of excess reagents from the reaction mixture, enabling reliable quantitative analysis of monosaccharides in hydrolysates of several glycoproteins. This separation mode is also applicable to oligosaccharides that are released from glycoproteins. The separation conditions are also applicable to other labeled saccharides. Therefore, our methods are applicable to most

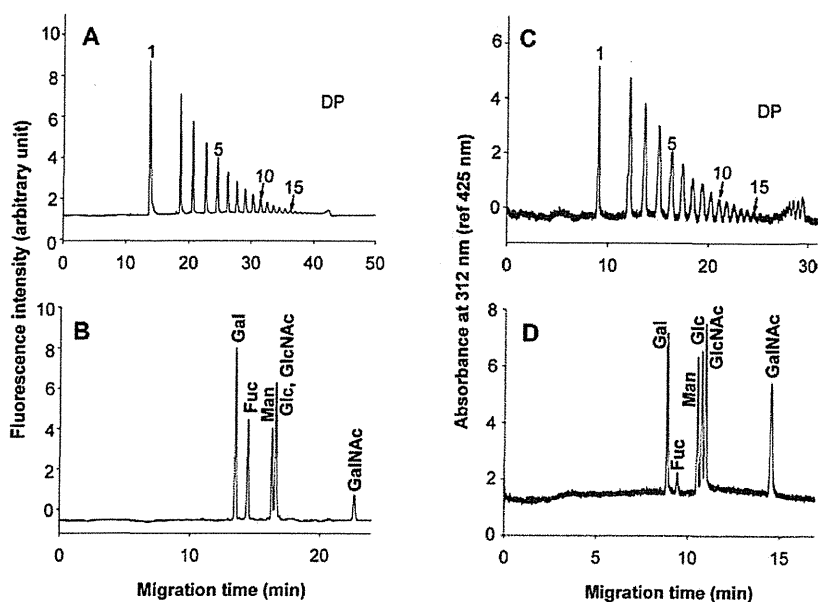


Figure 6. Application to the separation of isomaltooligosaccharides and monosaccharide mixtures labeled with AMAC (A, B) and ABEE (C, D). Analytical conditions for (A) and (C) were the same as those for Fig. 3 (A, B), while those for (B) and (D) were the same as those for Fig. 1 (B). AMAC derivatives were detected at 488 (ex)/522 (em) nm. ABEE derivatives were monitored by absorption at 210 nm.

reductively aminated saccharides, using neutral or basic labeling dyes without interference by excess reagents.

This work was supported by a Grant-in-Aid for Scientific Research (C) from the Japan Society for the Promotion of Science (JSPS), Japan, 2007–2011.

The authors have declared no conflict of interest.

5 References

- Anumula, K. R., *Anal. Biochem.* 2006, **350**, 1–23.
- Harvey, D. J., *J. Chromatogr.* 2011, **B 879**, 1196–1225.
- Vanderschaeghe, D., Festjens, N., Delanghe, J., Callewaert, N., *Biol. Chem.* 2010, **391**, 149–161.
- Briggs, J. B., Keck, R. G., Ma, S., Lau, W., Jones, A. J., *Anal. Biochem.* 2009, **389**, 40–51.
- Chen, F. T., Evangelista, R. A., *Electrophoresis* 1998, **19**, 2639–2644.
- Guttman, A., *Electrophoresis* 1997, **18**, 1136–1141.
- Huang, Y., Mechref, Y., Novotny, M. V., *Anal. Chem.* 2001, **73**, 6063–6069.
- Yagi, Y., Yamamoto, S., Kakehi, K., Hayakawa, T., Ohyama, Y., Suzuki, S., *Electrophoresis* 2011, **32**, 2979–2985.
- Hase, S., Ikenaka, T., Matsushima, Y., *J. Biochem.* 1981, **90**, 407–414.
- Nakagawa, H., Kawamura, Y., Kato, K., Shimada, I., Arata, Y., Takahashi, N., *Anal. Biochem.* 1995, **226**, 130–138.
- Takahashi, N., Khoo, K. H., Suzuki, N., Johnson, J. R., Lee, Y. C., *J. Biol. Chem.* 2001, **276**, 23230–23239.
- Tomiya, N., Kurono, M., Ishihara, H., Tejima, S., Endo, S., Arata, Y., Takahashi, N., *Anal. Biochem.* 1987, **163**, 489–499.
- Yodoshi, M., Oyama, T., Masaki, K., Kakehi, K., Hayakawa, T., Suzuki, S., *Anal. Sci.* 2011, **27**, 395–400.
- Yodoshi, M., Tani, A., Ohta, Y., Suzuki, S., *J. Chromatogr. A* 2008, **1203**, 137–145.
- Honda, S., Suzuki, S., *Anal. Biochem.* 1984, **142**, 167–174.
- Birrell, H., Charlwood, J., Lynch, I., North, S., Camilleri, P., *Anal. Chem.* 1999, **71**, 102–108.
- Wang, W. T., Ledonne, N. C., Ackerman, B., Sweeley, C. C., *Anal. Biochem.* 1984, **141**, 366–381.
- Suzuki, S., Honda, S., *Electrophoresis* 1998, **19**, 2539–2560.
- Hoffstetter-Kuhn, S., Paulus, A., Gassmann, E., Widmer, H. M., *Anal. Chem.* 1991, **63**, 1541–1547.
- Honda, S., Suzuki, S., Kakehi, K., *J. Chromatogr.* 1981, **226**, 341–350.
- Fournet, B., Montreuil, J., Strecker, G., Dorland, L., Haverkamp, J., Vliegenthart, J. F. G., Binette, P., Schmid, K., *Biochemistry* 1978, **17**, 5206–5214.
- Nakano, M., Kakehi, K., Tsai, M. H., Lee, Y. C., *Glycobiology* 2004, **14**, 431–441.
- Townsend, R. R., Hardy, M. R., Cumming, D. A., Carver, J. P., Bendiak, B., *Anal. Biochem.* 1989, **182**, 1–8.
- Spiro, R. G., Bhoyroo, V. D., *J. Biol. Chem.* 1974, **249**, 5704–5717.
- Green, E. D., Adelt, G., Baenziger, J. U., Wilson, S., Van Halbeek, H., *J. Biol. Chem.* 1988, **263**, 18253–18268.
- Tai, T., Yamashita, K., Ito, S., Kobata, A., *J. Biol. Chem.* 1977, **252**, 6687–6694.
- Tai, T., Yamashita, K., Ogata-Arakawa, M., Koide, N., Muramatsu, T., Iwashita, S., Inoue, Y., Kobata, A., *J. Biol. Chem.* 1975, **280**, 8569–8575.
- Yamashita, K., Tachibana, Y., Kobata, A., *J. Biol. Chem.* 1978, **253**, 3862–3869.
- Koller, A., Khandurina, J., Li, J., Kreps, J., Schieltz, D., Guttman, A., *Electrophoresis* 2004, **25**, 2003–2009.
- Honda, S., Akao, E., Suzuki, S., Okuda, M., Kakehi, K., Nakamura, J., *Anal. Biochem.* 1989, **180**, 351–357.

Common Glycoproteins Expressing Polylactosamine-Type Glycans on Matched Patient Primary and Metastatic Melanoma Cells Show Different Glycan Profiles

Mitsuhiro Kinoshita,[†] Yosuke Mitsui,[†] Naotaka Kakoi,[†] Keita Yamada,[†] Takao Hayakawa,[‡] and Kazuaki Kakehi^{*,†}

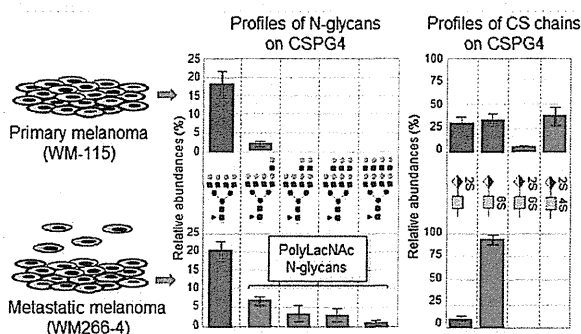
[†]School of Pharmacy, Kinki University, Kowakae 3-4-1, Higashi-Osaka 577-8502, Japan

[‡]Pharmaceutical Research and Technology Institute, Kinki University, Kowakae 3-4-1, Higashi-Osaka 577-8502, Japan

Supporting Information

ABSTRACT: Recently, we reported comparative analysis of glycoproteins which express cancer-specific *N*-glycans on various cancer cells and identified 24 glycoproteins having polylactosamine (polyLacNAc)-type *N*-glycans that are abundantly present in malignant cells [Mitsui et al., *J. Pharm. Biomed. Anal.* 2012, 70, 718–726]. In the present study, we applied the technique to comparative studies on common glycoproteins present in the matched patient primary and metastatic melanoma cell lines. Metastatic melanoma cells (WM266-4) contained a large amount of polyLacNAc-type *N*-glycans in comparison with primary melanoma cells (WM115). To identify the glycoproteins expressing these *N*-glycans, glycopeptides having polyLacNAc-type *N*-glycans were captured by a *Datura stramonium* agglutinin (DSA)-immobilized agarose column. The captured glycopeptides were analyzed by LC/MS after removing *N*-glycans, and some glycoproteins such as basigin, lysosome-associated membrane protein-1 (LAMP-1), and chondroitin sulfate proteoglycan 4 (CSPG4) were identified in both WM115 and WM266-4 cells. The expression level of polyLacNAc of CSPG4 in WM266-4 cells was significantly higher than that in WM115 cells. In addition, sulfation patterns of chondroitin sulfate (CS) chains in CSPG4 showed dramatic changes between these cell lines. These data show that characteristic glycans attached to common proteins observed in different stages of cancer cells will be useful markers for determining degree of malignancies of tumor cells.

KEYWORDS: polylactosamine, chondroitin sulfate, melanoma, malignant transformation



INTRODUCTION

Glycosylation is one of the frequently observed post-translational modifications of proteins and plays various important roles such as protein folding, cellular communications, and signal transductions.^{1,2} It is also well-known that embryonic development and cellular activation in mammalian cells are often accompanied by alterations in glycosylation. In addition, aberrant glycosylation has been known to be associated with various human diseases.^{3–7} Expression of GlcNAc transferase V (GlcNAcT-V), which is the rate-limiting enzyme for the synthesis of polylactosamine (tandem repeating units of Gal β 1-4GlcNAc at the nonreducing terminal ends), is increased in numerous cancer cells to cause increases of polyLacNAc-carrying *N*-glycans.^{8–11} Colon cancer cells highly express sialyl-Lewis^x (NeuAc α 2-3Gal β 1-4[Fuc α 1-3] GlcNAc-R), while they show markedly decreased level of sialyl 6-sulfo Lewis^x compared with normal colonic cells.¹² Thus, alterations in glycosylation are a universal hallmark and prominent biomarkers for cancer.

Serological assays detect carbohydrate antigens such as sialyl-Le^x, sialyl-Le^a (CA19-9) and MUC16 (CA125). Sialyl-Le^x is a weak marker for some small-cell lung cancers (24% for all stages), however, sialyl-Le^x increases with tumor progression (71% for late-stage).¹³ Unfortunately, elevation of these carbohydrate antigens is only suggestive of a cancer. α -Fetoprotein (AFP) is a well-known biomarker for liver diseases (e.g., cirrhosis, hepatitis, and hepatocellular carcinoma (HCC)), but its specificity for diagnosis of HCC is low (less than 50%). In contrast, fucosylated AFP (AFP-L3) is particularly useful in early detection of aggressive tumors associated with HCC with high specificity (>95%).¹⁴ Alteration of serum α 1-acid glycoprotein (AGP) has been reported to be associated with a risk of developing HCC during cirrhosis in chronic hepatitis. Kuno et al. statistically evaluated the relationship between the progression of liver fibrosis during cirrhosis and the decreased

Received: October 8, 2013

Published: December 19, 2013



α 2–3 sialylation/the increased core α 1-6fucosylation of *N*-glycans in AGP.¹⁵

Although time-consuming and laborious analysis is required for finding a candidate for cancer-specific biomarkers, detailed analysis of glycans in glycoconjugates provides us useful information for the development of novel biomarkers. In our previous reports, we proposed a series of methods for the analysis of glycans of glycoproteins in cancer cells.^{16,17} Total glycan pool obtained from the cells was fluorescently labeled with 2-aminobenzoic acid (2-AA) and separated based on the number of sialic acid residues attached to the glycans using affinity chromatography on a serotonin-immobilized stationary phase. Total amounts of glycans as well as those of each category of glycans (asialo/high-mannose, mono-, di-, tri-, and tetra-sialoglycans) were determined based on their fluorescent intensities. This is very important information for determination of the expressed level of each category of the glycans. Then, the collected glycan groups were extensively analyzed by MSⁿ technique. On the basis of the studies using these techniques, we found that histiocytic lymphoma cells (U937), kidney glandular cells (ACHN), gastric cancer cells (MKN45), and lung cancer cells (A549) express a large amount of *N*-glycans having polyLacNAc residues.^{16,17} To confirm glycoproteins which express these characteristic polyLacNAc-type *N*-glycans in cancer cells, tryptic-digested glycopeptides carrying multiple LacNAc units were captured using a *Datura stramonium* agglutinin (DSA)-immobilized column. The positions of peptides and glycans of the captured glycopeptides were analyzed by LC/MSⁿ-based technique after digestion with *N*-glycoamidase F, and we found that some glycoproteins such as CD107a and CD107b commonly contained polyLacNAc-type *N*-glycans in all the examined cancer cells. But integrin- α 5 (CD49e) and carcinoembryonic antigen-related cell adhesion molecule 5 (CD66e) having these glycans were specifically found in U937 and MKN45 cells, respectively. These data indicate that specific glycans attached to specific proteins will be promising markers for specific tumors with high accuracy.¹⁸

Melanoma consists of an invasive tumors that are resistant to conventional therapy.¹⁹ Therefore, monitoring of high-risk patients at early stage is highly recommended, but biomarkers for melanoma identification, prediction of progression, and prognosis are lacking. Although measurement of serum lactate dehydrogenase (LDH) is used for staging of melanoma, it is not specific for melanoma and cannot be used to predict progression or prognosis.¹⁹ Melanoma inhibitory activity (MIA), a 11 kDa soluble protein, is present in the supernatant of the human melanoma cell line (HTZ-19). However, increased MIA levels are also observed in a subset of the patients with ovarian, pancreatic, breast, and colon cancer.²⁰ 5-S-Cysteinyl-dopa (5-S-CD) is produced in melanocytes and melanoma cells and has been reported to be raised particularly in late-stage (stage III and IV).²⁰ Thus, these biomarkers are detected frequently in the advanced stages of melanomas but are not useful for monitoring of stages or early detection of melanoma progression.

In the present study, we performed comparative studies on common glycoproteins present in the matched patient primary and metastatic melanoma cell lines, WM115 and WM266-4. At the initial step, total *N*-glycans expressed in both melanoma cells were comprehensively analyzed. Subsequently, glycoproteins having characteristic *N*-glycans that were observed in both cell lines were identified by combination of lectin-affinity capturing and bottom-up proteomics approaches. Among

identified glycoproteins, chondroitin sulfate proteoglycan 4 (CSPG4) having both *N*-glycans and glycosaminoglycans (GAGs) was confirmed as a convincing marker for the melanoma-specific glycoproteins, and the structures of *N*-glycans and glycosaminoglycans of CSPG4 from each cell line were studied in detail.

MATERIALS AND METHODS

Materials

Peptide *N*-glycoamidase F (EC 3.5.1.52) was obtained from Roche Diagnostics (Mannheim, Germany). Neuraminidase (*Arthrobacter ureafaciens*) was kindly donated by Dr. Ohta (Marukin-Bio, Uji, Kyoto, Japan). Benzonase was obtained from Novagen (Darmstadt, Germany). TPCK-treated trypsin was from Worthington (Lakewood, NJ). Anti-LAMP-1 (H4B3) mouse IgG1 monoclonal, and anti-CSPG4 (LHM2) mouse IgG monoclonal were from Santa Cruz Biotechnology (Santa Cruz, CA). Anti-Basigin (MEM-M6/1) mouse IgG1 monoclonal was from Abcam (Cambridge, U.K.). Iodoacetamide was from Tokyo Kasei Kogyo (Chuo-ku, Tokyo, Japan). Dithiothreitol (DTT) was obtained from Nacalai Tesque (Nakagyo-ku, Kyoto, Japan). 3,3'-Diaminobenzidine tetrahydrochloride (DAB) was obtained from DOJINDO (Kamimashiki-gun, Kumamoto, Japan). 2-Aminobenzoic acid (2-AA) and sodium cyanoborohydride for fluorescent labeling of oligosaccharides were from Tokyo Kasei. Coomassie brilliant blue G-250 was purchased from BIO-RAD (Hercules, CA). Sephadex LH-20 was from Amersham Bioscience (Uppsala, Sweden). Vivaspin 500 was obtained from Sartorius (Goettingen, Germany). *Datura stramonium* agglutinin (DSA)-agarose, chondroitinase ABC, and standard samples of unsaturated disaccharides derived from glycosaminoglycans were obtained from Seikagaku Kogyo (Chuoku, Tokyo, Japan). VECTA Elite ABC mouse IgG kit for Western blotting was obtained from Vector Laboratories (Burlingame, CA). Immobilon-P transfer membrane (PVDF) was from Millipore (Bedford, MA). Protein inhibitor cocktail for animal cells was obtained from Nacalai Tesque. Protein G Sepharose 4 Fast Flow was obtained from GE Healthcare (Uppsala, Sweden). All other reagents and solvents were of the highest grade commercially available or of HPLC grade. All aqueous solutions were prepared using water purified with a Milli-Q purification system (Millipore, Bedford, MA).

Cell Culture

WM266-4 (human metastatic melanoma cells) and WM115 cells (human primary melanoma cells) derived from a same patient were employed as the materials. Both cells were cultured at 37 °C under 5% CO₂ atm in EMEM medium supplemented with 10% (v/v) fetal bovine serum, 2 mM glutamine, 1% nonessential amino acids (NEAA), and 1% sodium pyruvate. The cells were harvested at 80% confluent state, washed with phosphate buffered saline (PBS), and collected by centrifugation at 1000 rpm for 20 min.

Whole Proteins from Melanoma Cell Lines

Melanoma cells (1.0 × 10⁷ cells) were suspended in PBS (50 μ L) containing 1 mM EDTA and kept at room temperature for 15 min. Extraction reagent (7 M urea, 2 M thiourea, 4% CHAPS, 30 mM Tris-HCl (pH 8.5, 268 μ L)), 1 M DTT (17 μ L), and benzonase (125 units, 5 μ L) were added to the suspended cells and kept at 37 °C for 30 min. The mixture was centrifuged at 8000g for 15 min. After addition of acetone